

T-2862

STRUCTURAL FEATURES OF A LARAMIDE FOLD AND THRUST BELT,
EAST FLANK OF THE SANGRE DE CRISTO RANGE, COLORADO

by
Gabrielle Schavran

ProQuest Number: 10782558

All rights reserved

INFORMATION TO ALL USERS

The quality of this reproduction is dependent upon the quality of the copy submitted.

In the unlikely event that the author did not send a complete manuscript and there are missing pages, these will be noted. Also, if material had to be removed, a note will indicate the deletion.



ProQuest 10782558

Published by ProQuest LLC (2018). Copyright of the Dissertation is held by the Author.

All rights reserved.

This work is protected against unauthorized copying under Title 17, United States Code
Microform Edition © ProQuest LLC.

ProQuest LLC.
789 East Eisenhower Parkway
P.O. Box 1346
Ann Arbor, MI 48106 – 1346

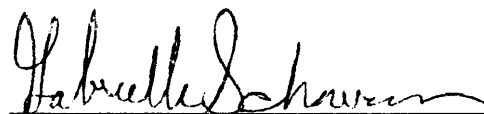
T-2862

A thesis submitted to the Faculty and the Board of Trustees of the Colorado School of Mines in partial fulfillment of the requirements for the degree of Master of Science (Geology)

Golden, Colorado

Date 4/16/84

Signed:



Gabrielle A. Schavran

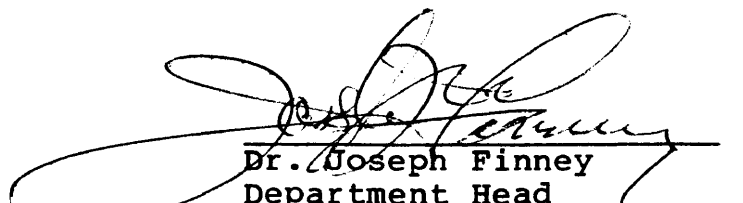
Approved:



Eric P. Nelson
Thesis Advisor

Golden, Colorado

Date 4/16/84



Dr. Joseph Finney
Department Head
Department of Geological
Engineering

ABSTRACT

Laramide deformation has resulted in a fold and thrust belt within the Pennsylvanian Minturn Formation along the east flank of the Sangre de Cristo Range, Colorado. An imbricate thrust system and associated major folds and minor structures were mapped west of the town of Chama.

Thrusts dip 5 to 15 degrees to the west. Minor tear faults offset the thrust faults along strike. Major folds are inclined to overturned near the leading edges of the thrusts. The folds become open and diminish in amplitude to the west. Minor thrust faults are present in the hinge regions of some of the anticlines. Fold axes trend between N10W-N60W and plunge gently to the northwest and southeast. The direction of tectonic transport is interpreted to be southwest to northeast, or perpendicular to the major fold trends.

Mesoscopic structures include small bedding-plane thrusts, parasitic folds, reverse faults, normal faults, joints, and slickensides. Bedding-plane thrusts also indicate shortening in the southwest to northeast direction. Mesoscopic folds trend northwest-southeast and plunge up to fifty degrees to the northwest and southeast. The strike of the reverse faults are parallel to the trends of the fold

axes. Extension joints and normal faults trend northeast-southwest and locally crosscut the bedding thrusts.

The structures formed as follows: A major compressional event during the Laramide orogeny transported a number of imbricate thrust sheets from the southwest to northeast, probably above a major decollement surface. Folds, mesoscopic bedding-plane thrusts, reverse faults and tear faults developed during the thrusting and imbrication. Mesoscopic normal faults are related to relaxation or extension after the thrusting event. Precambrian rocks to the west are believed to be allochthonous suggesting that the fold and thrust belt represents a zone of Laramide crustal shortening.

TABLE OF CONTENTS

	<u>page</u>
ABSTRACT.iii
TABLE OF CONTENTS	v
LIST OF FIGURES AND TABLES.	viii
LIST OF PLATES	x
ACKNOWLEDGEMENTS.	xi
INTRODUCTION.	1
Location	1
Topography and Drainage.	1
Purpose and Scope of Research.	4
Procedures	4
Previous Work.	6
Geologic Setting	7
STRATIGRAPHY.	11
Introduction	11
Lower Clastic Unit	16
Middle Carbonate Unit.	17
Upper Clastic Unit	19
STRUCTURAL GEOLOGY.	20
Regional Structural Setting.	20
Macroscopic Structural Features.	22
Introduction.	22

TABLE OF CONTENTS (continued)

	<u>page</u>
Lower Plate	24
Thrust Faults.	24
Folds.	25
Middle Plate.	29
Thrust Faults.	29
Reverse Faults	30
Tear Faults.	33
Folds.	34
Upper Plate	36
Thrust Faults.	38
Folds.	40
Summary	40
Mesoscopic Structural Features	42
Introduction.	42
Mesoscopic Thrusts.	42
Folds	44
High-Angle Faults	45
Joints.	49
Slickensides.	50
Summary	51
Microfabrics	52

TABLE OF CONTENTS (continued)

MODEL FOR THE GENESIS OF STRUCTURES	56
CONCLUSIONS	61
REFERECNCES CITED.63

LIST OF FIGURES AND TABLES

<u>Figure</u>	<u>Page</u>
1. Location of field area	2
2. Field area in detail	3
3. Ancestral Rocky Mountain uplifts and basins.	9
4. Generalized stratigraphic column	12
5. Correlation chart of stratigraphic terminology within Huerfano Park.	14
6. Regional geologic map.	21
7. Major structures in field area	23
8. Development of thrust fault between lower and middle plate.	26
9. Lower plate geology.	27
10. PI-diagram of major folds in field area.	28
11. Antiformal syncline in middle plate.	31
12. Schematic cross section exemplifying the style of thrusting in a fold hinge.	32
13. PI-diagrams of large anticline in middle plate.	35
14. Propeller like fold.	37
15. Longitudinal section x-x'.	39
16. PI-diagram of open syncline in upper plate.	41
17. Photograph of minor thrust fault	43
18. Photograph of minor fold	46

LIST OF FIGURES AND TABLES (continued)

19. Modified flexural fold 47
20. Drag along a minor normal fault. 48
21. Sample locations 53
22. Diagramatical model for the formation. 57
of large thrust faults in the Huerfano
Park area.

<u>Table</u>	<u>page</u>
1. Petrographic descriptions.	55

LIST OF PLATES

- I Geologic map and structure sections.in pocket
- II Structure map.in pocket
- III Bedding map.in pocket
- IV Synthesis of mesoscopic fabrics.in pocket

ACKNOWLEDGEMENTS

I would like to thank ARCO Oil Company, Mobil Oil Company, Chevron Oil Company, Sigma Xi, and the Colorado School of Mines for their financial support in my research. A special thanks to Dr. Eric P. Nelson, my advisor, for considerable time and advice throughout the course of this study. Dr. R.H. De Voto and Dr. J. Geissman were helpful and supportive as committee members. David Lindsey of the U.S.G.S., and Dr. Erle Kauffman of the University of Colorado contributed advice and supplies for my study. Dr. R.H. De Voto and David Lindsey were helpful in the field. S.F. Thompson was a wonderful field assistant and friend. Dr. R.A. Jackson was most helpful in every way, and Jackson Schavran gave his support.

INTRODUCTION

Location

The study area, located in T.27S., R.71W., south-central Colorado (Fig. 1), is in Huerfano county, eleven kilometers (seven miles) west of the town of Gardner, south of Route #150. The area is located in Huerfano Park which is bounded on the west by the Sangre de Cristo Range, on the east by the Wet Mountains, on the north by the Wet Mountain Valley, and opens south to the high plains (Fig. 1). Access to the study area includes Highway 69, Route #150, and numerous unnamed dirt roads in the Redwing-Chama area. Locally, the area is bounded by the Huerfano River on the north, the Manzanares Creek on the west, the Martin Creek on the south, and by the village of Chama on the east (Fig. 2).

Topography and Drainage

Topography in the study area is moderately rugged with elevations ranging from 8,200 to 9,272 feet. Of the five streams that drain eastward, the Martin Creek is the only perennial stream. The Manzanares Creek and Huerfano River

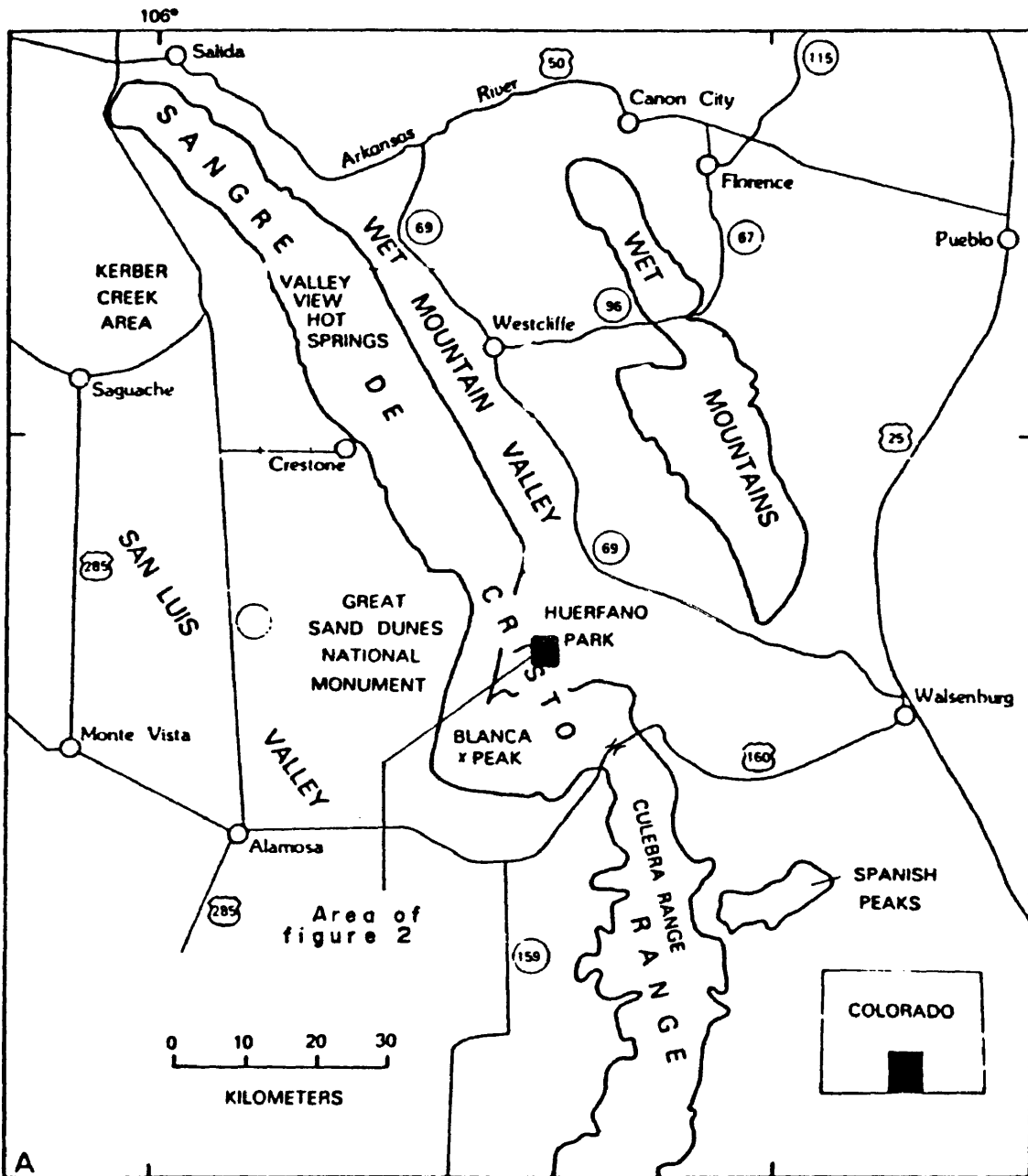


Figure 1. Location of thesis area (from Lindsey et al., 1983).

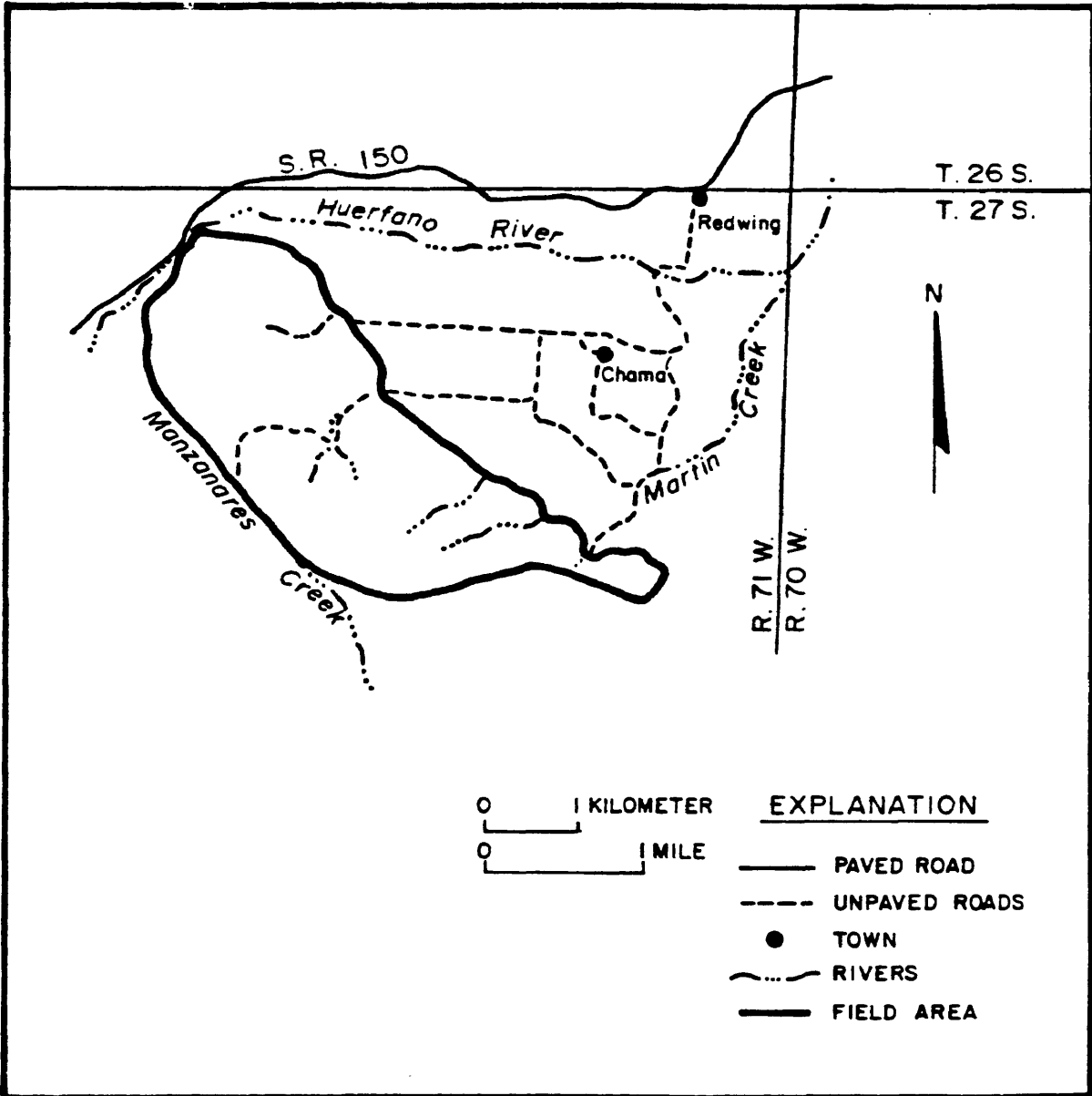


Figure 2. Study area in detail.

drain the high peaks of the Sangre de Cristo Range and the higher hills of the western slope of the study area (Fig. 2).

Purpose and Scope of Research

This study is a detailed structural analysis of part of a Laramide overthrust belt located on the east flank of the Sangre de Cristo Range. Geologic mapping and measurement of mesoscopic structural features including folds, faults, and joints were used to define geometric relationships and the style of deformation in the area. The objective of this study is to describe the types of structures and to produce a model for their development in this fold and thrust belt which can be applied to the understanding of other areas with similar deformational styles and histories.

Procedures

The investigation comprised the following field work and laboratory and office research.

A) Field Work

- 1) Eight weeks of detailed mapping of an 8 square

kilometer area at a scale of 1:12,000 using topographic maps and aerial photographs

- 2) Description of mappable units and compilation of a generalized stratigraphic section for the study area
- 3) Mapping and measurement of minor structural features such as: folds, thrust faults, high-angle faults, slickensides, and joints
- 4) Collection of oriented samples from key locations for thin section analysis

B) Laboratory and Office Research

- 1) Compilation and analysis of mesoscopic structural data displayed on equal-area nets and on a series of structural maps
- 2) Construction of cross sections through the field area to display the major structures
- 3) Description of structural geometries and the interpretation of genesis of the structures
- 4) Thin section analysis of a carbonate marker bed for determination of microscopic strain
- 5) Development of Kinematic model

Previous Work

Endlich (1877) and Bagg (1908) conducted the earliest studies in the area and believed the Sangre de Cristo Range to be a large anticline with Pennsylvanian sedimentary rocks covering a Precambrian core. Johnson (1929) conducted the first detailed geologic study of the Sangre de Cristo Range. Burbank and Goddard (1937) mapped the macroscopic structures in Huerfano Park and believed thrusting was related to the formation of the Sangre de Cristo Range. Gableman (1952), Karig (1964), Litsey (1958), Burford (1960), and Volkman (1965) investigated the structure and origin of the northern Sangre de Cristo Range. Students from the University of Michigan mapped the Huerfano Park area in the late 1950's and a compilation of the work is nearly completed (Kauffman, 1983, oral communication).

Smith (1961) mapped the geology of the Redwing area and his geologic map was used as a reference during the present investigation. However, because of the large area he covered, mapping revisions were necessary to understand the detailed structural geometries of the area.

Brill (1952) conducted a detailed study of the Permian and Pennsylvanian sedimentary rocks from northern New Mexico through Colorado. Bolyard (1959), Rhodes (1960), Pierce

(1969), and Taranik (1974) provided information on the stratigraphy of the surrounding area. The Pennsylvanian stratigraphy and faunal zonation of the Huerfano Park area was reported by Tischler (1961). Tischler's study was most helpful for the determination of the units mapped in the present study. In addition, De Voto (1980) and De Voto and Peel (1972) discussed the Pennsylvanian stratigraphy of Colorado, and Clarke (1982) studied the Des Moinesian upper part of the Minturn Formation in the Crestone area.

Johnson (1960) mapped the geology and described the mechanisms of deformation in Huerfano Park. Munger (1965) and Lindsey et al. (1983) have studied the large-scale structures in the Sangre de Cristo Range. These works are most helpful for the understanding of the regional tectonic setting.

Geologic Setting

The field area is located on the east flank of the Precambrian-cored Sangre de Cristo Range. Pennsylvanian sedimentary rocks which have been thrust faulted and folded are exposed in the area. To the east, Mesozoic and Tertiary rocks are deformed in a similar style. Precambrian rocks, exposed in the Sangre de Cristo Range and Wet Mountains, were

deposited as sedimentary rocks and subsequently underwent several episodes of metamorphism and igneous intrusion.

In the Crestone area (Fig. 1), a basal Ordovician sandstone lies unconformably on Precambrian rocks (Volkman, 1965). Early Paleozoic time was a period of tectonic quiescence. Transgression over an eroded Precambrian craton resulted in the deposition of Ordovician through Mississippian carbonates and interbedded clastics west of Huerfano Park and in the northern Sangre de Cristo Range.

The Ancestral Rocky Mountain event, which resulted in a series of uplifted mountain blocks and related, intervening basins, extended from Late Mississippian to Permian time. The Ancestral Rocky Mountain uplifts were large, northwest-trending, elongate, basement blocks bordered by deep asymmetrical basins (Fig. 3) (De Voto, 1980). The Huerfano Park area was part of the 644-kilometer-long Central Colorado trough. Beginning in Morrowan time and continuing through Virgilian time, up to 3050 meters of coarse- to fine-grained clastics were shed off the Ancestral Front Range and Sawatch uplifts (Fig. 3) and were deposited along the periphery of the Central Colorado trough (De Voto, 1980). Carbonates and evaporites were deposited in the deeper, marine environments within the basin. From Late Pennsylvanian through Permian time continuous, but slower, rates of uplift persisted in the

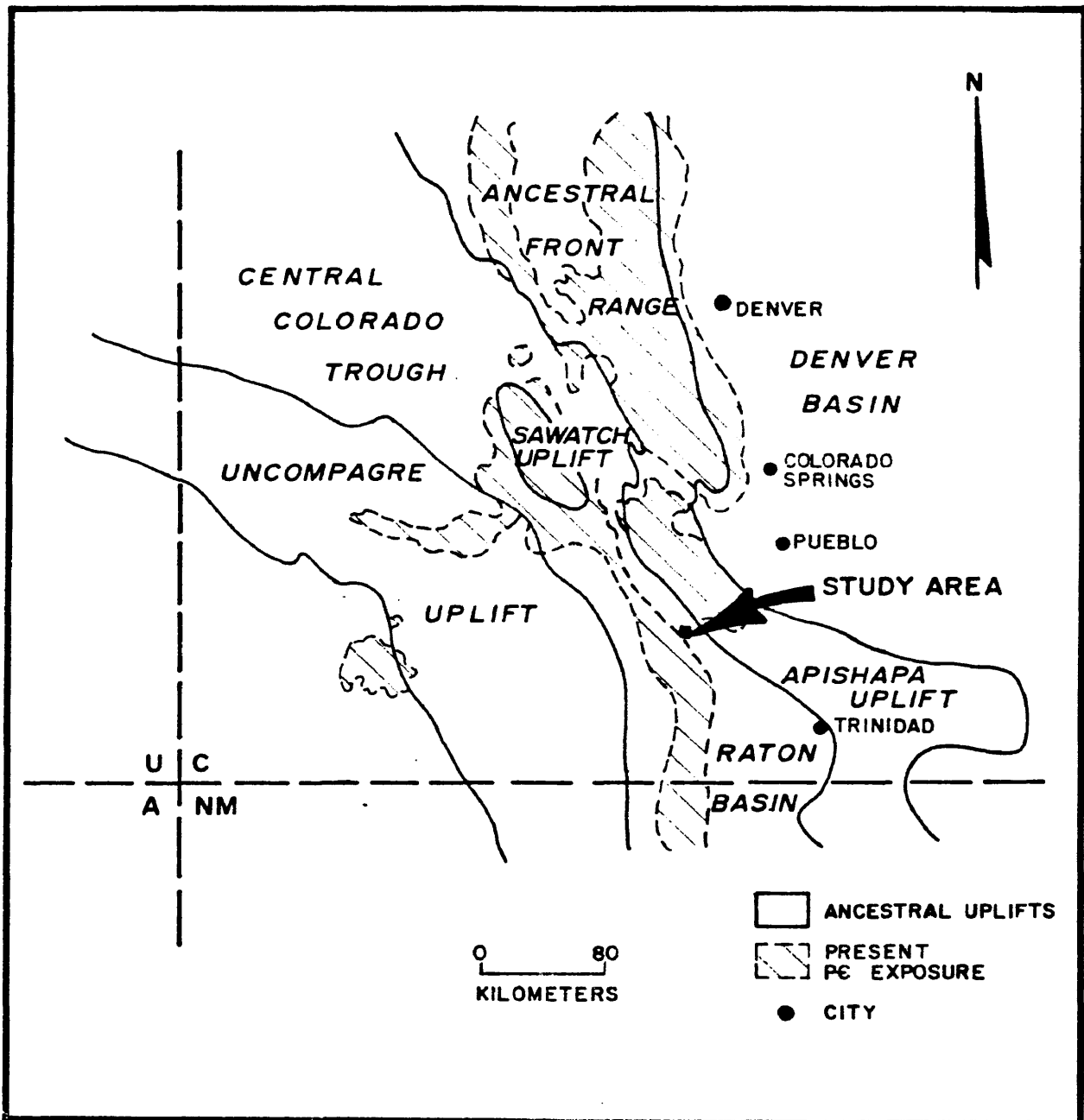


Figure 3. Ancestral Rocky Mountain uplifts and basins (From De Voto, 1980).

region (Mallory, 1975). A period of tectonic quiescence returned during early Mesozoic time, although some Jurassic and Cretaceous terrigenous nonmarine and marine sediments were deposited.

The present Sangre de Cristo Range began its development during the Laramide event that spans from the Late Cretaceous through Eocene time (Lindsey et al., 1983). The Sangre de Cristo Range and its structural features generally trend north-south and show evidence of eastward, and locally westward, thrusting. Paleozoic through Tertiary rocks in Huerfano Park have been thrust faulted and folded during this event.

Neogene uplift of the Sangre de Cristo Range and Wet Mountains formed the highlands seen today (Lindsey et al., 1983). The Wet mountain Valley-Huerfano Park basin is a Neogene graben which developed after late Oligocene igneous activity in the area (Lindsey, 1983). Periods of Quaternary glaciation, terracing, and erosion have carved the present topography.

STRATIGRAPHY

Introduction

Three mappable units within the Pennsylvanian Minturn Formation crop out in the area west of the town of Chama (Fig. 4). The lower clastic unit is a cyclic, braided, fan-delta deposit consisting of interbedded arkosic conglomerate, arkosic sandstone and siltstone, and calcarenite to arkosic limestone. At the top of the lower clastic unit a green arkosic sandstone grades into a green, argillaceous, lime packstone which marks the contact with the middle carbonate unit, a shelf carbonate sequence consisting of a basal, clay-rich, fossiliferous, lime packstone rich with Dictyoclostus brachiopods. This basal unit is overlain by fossiliferous lime packstone and wackestone and oolitic packstone. The oolitic packstone grades upward into an oolitic grainstone with quartz sand nuclei. The oolitic grainstone grades into the upper clastic unit which is a shallow marine sequence of shale, siltstone, and fine- to coarse-grained sandstone.

The lower clastic unit and member A of the middle carbonate unit have been variously referred to by previous workers as the Madera Formation (Brill, 1952; Bolyard, 1959; Tischler,

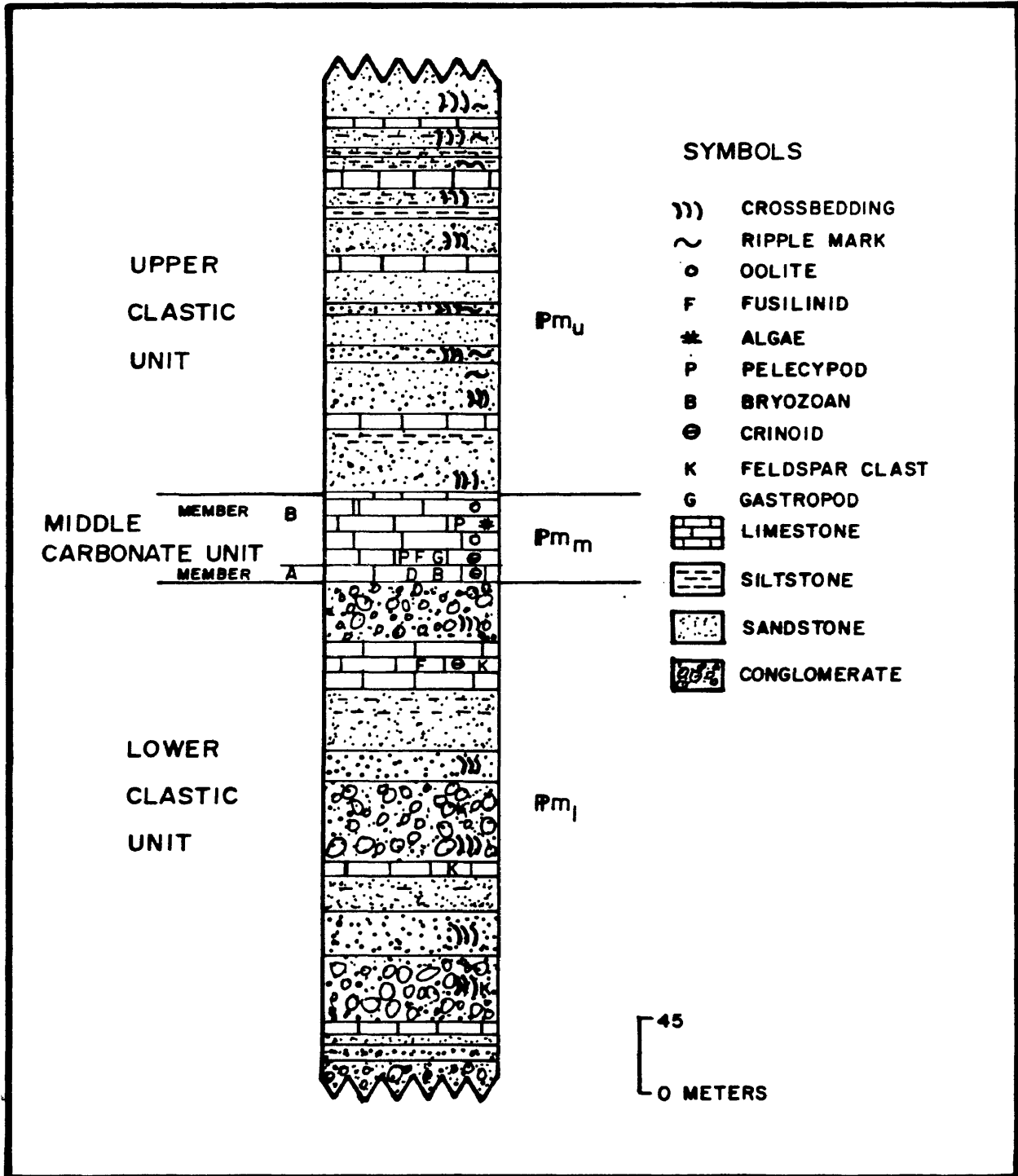


Figure 4. Generalized stratigraphic column for the upper portion of the Minturn Formation in the study area.

1960), the Hermosa Formation (Burbank and Goddard, 1937), and the lower unit of the Sangre de Cristo Formation (Smith, 1961). Member B of the middle carbonate unit has been referred to as the Whiskey Creek Pass Limestone of the Madera Formation (Brill, 1952; Bolyard, 1959; and Tischler, 1960), the Rico Formation (Burbank and Goddard, 1937), and the oolitic limestone member of the lower unit of the Sangre de Cristo Formation (Smith, 1961). The upper clastic unit has been previously termed the Sangre de Cristo Formation (Burbank and Goddard, 1937; Brill, 1952), the Pass Creek Formation (Bolyard, 1959), and Pass Creek beds of the Madera Formation (Tischler, 1960), and the upper unit of the Sangre de Cristo Formation (Smith, 1961).

Although the term Madera is used as the Minturn equivalent in northern New Mexico and southern Colorado (Bolyard, 1959), more recent studies throughout the Sangre de Cristo Range have used the term "Minturn Formation" instead of the term "Madera" (Clarke, 1983; Lindsey et al., 1984, in press). Following this modern usage, the stratigraphy has been subdivided into three mappable units within the Minturn Formation. Figure 5 is a correlation chart comparing stratigraphic nomenclature for the Pennsylvanian rocks of the study area.

Figure 5. Correlation chart of stratigraphic terminology within Huerfano Park.

SERIES	BURBANK AND GODDARD 1937	BRILL 1952	BOLYARD 1959	TISCHLER 1960	SMITH 1961	THIS STUDY	
DES MOINESIAN	SANGRE DE CRISTO FORMATION	SANGRE DE CRISTO	SANGRE DE CRISTO FM.	SANGRE DE CRISTO FM.	SANGRE DE CRISTO FORMATION	UPPER CLASTIC UNIT	
	CONGLOMERATIC BEDS		LOWER MEMBER	PASS CREEK BEDS			
	RICO FORMATION	WHISKEY CREEK PASS LIMESTONE	WHISKEY CREEK PASS LIMESTONE	WHISKEY CREEK PASS LIMESTONE	UPPER UNIT	MIDDLE CARBONATE UNIT	
	HERMOSA FORMATION	MADERA FORMATION	ARKOSIC LIMESTONE MEMBER	DICTYOCLOSTUS BED	DICTYOCLOSTUS BED	LOWER UNIT	MEMBER B
				MEMBER A			
	HERMOSA FORMATION	MADERA FORMATION	ARKOSIC LIMESTONE MEMBER	MADERA FORMATION	MADERA FORMATION	SANGRE DE CRISTO FORMATION	LOWER CLASTIC UNIT

The reasons for considering most of the sequence to be a part of the Minturn Formation rather than a portion of the overlying Sangre de Cristo Formation are outlined below. Several Sections of the Madera (Minturn) Formation were analyzed by Tischler (1961) from La Veta Pass to Chama. Tischler's thesis (1961) is the most recent detailed analysis of Pennsylvanian stratigraphy in western Huerfano Park, and his correlations have been used to determine the generalized stratigraphy of this study. Tischler (1961) places the contact between the Madera and the Sangre de Cristo Formations above the Pass Creek beds of the Madera Formation. The upper clastic unit in the field area may be interpreted to be a portion of the Pass Creek beds, thus the base of the Sangre de Cristo Formation may be stratigraphically above the upper clastic unit mapped in the study area. Moreover, the color of the sandstones in the lower and upper clastic units resembles Minturn sandstones in other areas along the Sangre de Cristo Range where the Minturn sandstones are dominantly gray and green, rather than the red color of the Sangre de Cristo sandstones (De Voto, 1980; Lindsey, 1983, oral communication). In addition, a Middle Des Moinesian age was determined for the lower clastic unit and the middle carbonate unit by fusilinid identifications (Beedeina sp.) (Douglass, 1983, written communication). This age corres-

ponds to the age of the Minturn Formation in the Crestone area (Clarke, 1982), and the Madera Formation in southern Colorado (Bolyard, 1959). Brill (1952), and Bolyard (1959) interpret the Sangre de Cristo Formation to be generally Wolfcampian in age.

Lower Clastic Unit

The lower clastic unit is broadly characterized by sedimentary cycles. Each cycle consists of the following, from bottom to top: large-scale cross-bedded, graded, pink and green arkosic conglomerate; red weathering, cross-bedded, arkosic, coarse- to medium-grained sandstone; quartz, medium- to fine-grained sandstone; green siltstone; calcareous, green, micaceous, fine-grained sandstone; sandy, arkosic- to quartz-rich lime packstone and grainstone; and fossiliferous, arkosic grainstone and calcarenite (Fig. 4). The thickness of the cycles ranges from a few meters to approximately ten meters, and the total thickness is approximately 215 meters in the study area.

The environment of deposition is believed to be a migrating fan-delta system deposited along the edge of the Central Colorado trough basin during Pennsylvanian time (Clarke, 1982). This is consistent with Holmes' (1965) defi-

dition of fan-deltas as alluvial fans that prograde from an adjacent highland into a standing body of water. Each cycle represents the following sedimentary scenario: The coarse, arkosic sandstones and conglomerates are braided fan deposits. As the lobe of fan deposition migrates laterally, a fining-upward clastic sequence is deposited. Eventually, the area is completely abandoned and marine carbonate deposition occurs. As the fan shifts back, the cycle is repeated.

Middle Carbonate Unit

The middle carbonate unit has been subdivided and mapped as two members (Fig. 4). Member A is stratigraphically beneath member B throughout the study area.

Member A is a fossiliferous, nodular, gray- to green-weathering, carbonaceous, argillaceous, lime packstone or locally a wackestone. Fossils include crinoids, bryozoa, foraminifera, gastropods, and brachiopods. Several genera of brachiopods are present, but Dictyoclostus is the most abundant. Bedding is characteristically fissile, and the total thickness is approximately 12 meters. Member A is interpreted to have been deposited in a sheltered-marine embayment environment (Clarke, 1982).

Member B consists of a series of carbonate facies. Upward from the base the following sequence is observed: Fossiliferous (tetracorals, brachiopods, bryozoas), poorly layered, gray- to green, lime wackestone to packstone with micrite nodules; tan-weathering, sandy, lime wackestone; massive, gray- to tan-weathering, well-layered lime mudstone to wackestone; fossiliferous (tetracorals, pelecypods, gastropods) lime packstone; sandy, tan- to gray, oolitic, lime packstone to grainstone; and massive, gray-weathering, oolitic, lime grainstone. Locally, there are facies variations that include fusilinid-rich and green-algae-rich layers. Member B is approximately 46 meters thick.

Member B probably represents a shallow marine shelf carbonate sequence. It is a relatively widespread unit and may represent a rise in sea level, subsidence of the basin, or a combination of the two.

The middle carbonate unit includes the only mappable marker beds in the study area. Its lithologic consistency, stratigraphic position relative to the upper and lower clastic units, and the paired A and B members facilitated detailed geologic mapping. Member B of the middle carbonate unit is correlative to the Whiskey Creek Pass Limestone of the Madera Formation (Tischler, 1961) (Fig. 5).

Upper Clastic Unit

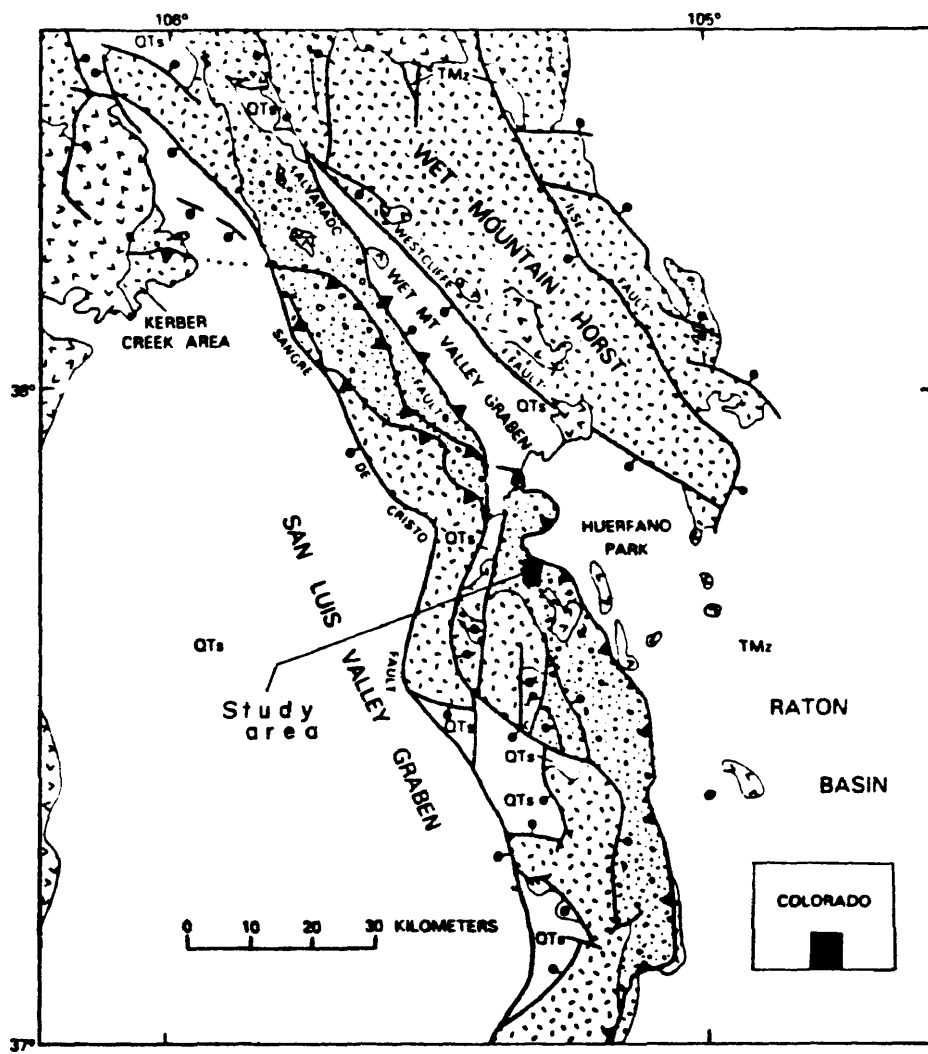
The upper clastic unit consists of calcareous, green, micaceous, medium- to fine-grained sandstone; reddish brown, silty, fine-grained sandstone with oscillation ripple marks; cross-bedded, massive to thin-bedded green sandstone; white-weathering, limy siltstones and shales; interbedded black shale and thin-bedded limestone with chert nodules; locally cross-bedded, tan-weathering, medium- to coarse-grained, friable sandstone; cross-bedded, limy, green, silty sandstones; and pink and green arkosic sandstones. Cycles were indeterminable because of frequent lateral facies changes. The total thickness of the upper clastic unit is approximately 190 meters.

The upper unit was probably deposited in a shallow-marine environment. The clastic influx is indicative of either a relative drop in sea level, a general increase in sediment influx, or a combination of the two.

STRUCTURAL GEOLOGY

Regional Structural Setting

The Sangre de Cristo Range is composed primarily of Precambrian crystalline and Upper Paleozoic sedimentary rocks. A thick sequence of Paleozoic, Mesozoic, and Cenozoic sedimentary rocks underlies the Huerfano Park area to the east (Johnson, 1964). The Paleozoic and Mesozoic rocks in the region have been folded and faulted during the Laramide event which is dated regionally as Late Cretaceous to Eocene (Lindsey et al., 1983). Large northwest-trending thrust plates form a belt extending from Huerfano Park to Valley View Hot Springs (Figs. 1 and 6). Total shortening near the 37° 45' latitude is estimated to be 14 kilometers (Lindsey et al., 1983). A Laramide age for the thrusting and folding in Huerfano Park is based on: 1) the presence of unconformities separating strongly folded rocks of Late Cretaceous age from gently folded rocks of Paleocene and younger age, 2) detritus derived from Paleozoic rocks in Eocene strata (Burbank and Goddard; 1937, Tweto, 1975), and 3) in the Redwing area (Fig. 2) regionally traceable Cretaceous marine sedimentary rocks have been tightly folded and thrust.



EXPLANATION

- QTs Quaternary and Upper Tertiary sediments
- Tertiary igneous rocks Tertiary igneous rocks
- TMz Lower Tertiary and Mesozoic sedimentary rocks
- Paleozoic sedimentary rocks Paleozoic sedimentary rocks
- Precambrian crystalline rocks Precambrian crystalline rocks
- Contact
- ▲ Major thrust fault
- ▼ Major normal fault

Figure 6. Geologic map of the northern Sangre de Cristo Range (from Lindsey et al., 1983).

The formation of structures within the Sangre de Cristo Range has been interpreted to be caused by: 1) uplift with peripheral thrusting (Burbank and Goddard, 1937; Tweto, 1975), 2) gravity sliding (Karig, 1964), 3) regional compression (Lindsey et al., 1983), 4) regional transcurrent movement (Sales, 1968), and 5) vertical uplift of basement blocks (Stearns, 1978; Matthews, 1976).

The Sangre de Cristo Range was uplifted during the Neogene, in association with extensional rift faulting which downdropped the San Luis and Wet Mountain valleys (Lindsey et al., 1983). The Sangre de Cristo horst probably began to rise in late Oligocene time (Lindsey et al., 1983).

Macroscopic Structural Features

Introduction

The rocks in the study area are exposed in three thrust plates. The lowermost, and possibly the oldest plate is exposed in the central part of the field area in a fenster (Fig. 7 and Pl. I). Although the basal thrust of this plate is nowhere exposed, its presence is inferred. In the northwest corner of the fenster the rocks are deformed into an overturned anticline plunging to the northwest (Pls. I, II, and III).

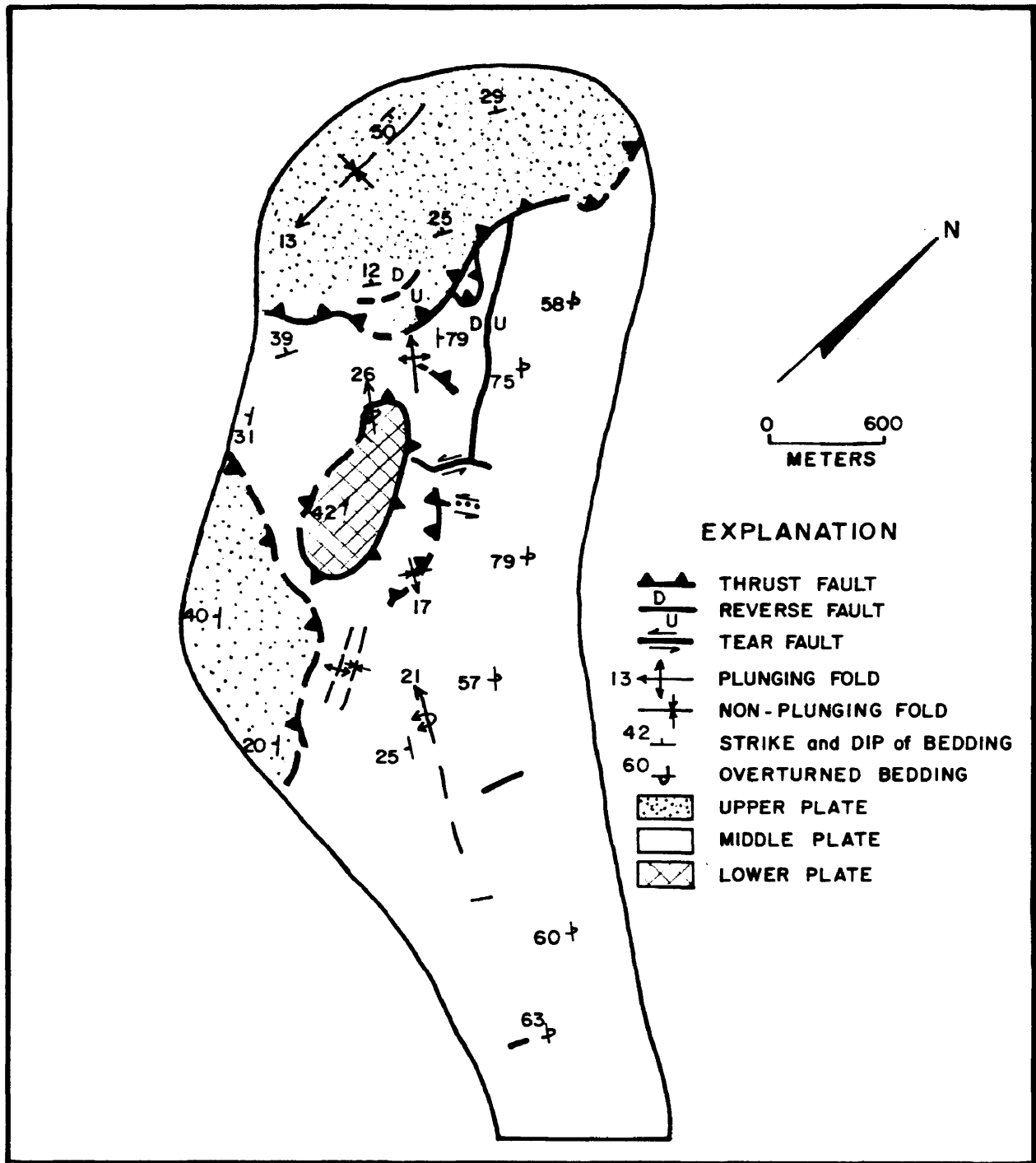


Figure 7. Major structures in the study area.

The middle plate is exposed over the length of the field area and contains several macroscopic structures related to the faulting. The main structure within the middle plate is a large, northwest-plunging anticline (Fig. 7, and Pls. I and II).

The upper plate, interpreted to be the youngest, is exposed in the western and northern portions of the field area (Fig. 7). Only the lower clastic unit of the Minturn Formation is exposed within the upper plate in the field area.

Lower Plate

The rocks of the lower plate, located in the central part of the field area (Pl. I), are exposed in a structural fenster covering approximately 372 square meters (4000 square feet). All three units of the Minturn Formation crop out in the lower plate. The strata trend northwest, and dip either steeply to the east or are overturned to the southwest (Pl. III).

Thrust Faults

The lower plate may be autochthonous or allochthonous. Inferred from the following criteria it is here considered allochthonous: 1) The beds throughout most of the plate are

overturned to the west indicating possible drag along a hidden thrust surface; and 2) east of the field area Cretaceous rocks are folded and thrust in a style similar to the style observed in the study area.

The thrust fault separating the lower plate from the middle plate is fairly well located along the eastern portion of the fenster (Pl. I). On the eastern side of the fenster solutions to a series of three point problems along different parts of the thrust fault give dips of 5-15 degrees east. On the western side of the fenster using the same method, dips of 12-18 degrees west were found. Although there is no evidence, it is postulated that the middle thrust plate developed as a result of shearing in the hinge region of a major syncline in the lower plate (Fig. 8). The thrust above the lower plate cuts down section on the eastern side of the fenster.

Folds

An overturned anticline is present in the northwest corner of the fenster (Figs. 7, 9, and P. II). The eastern, overturned limb dips 45-80 degrees west and makes up most of the fenster. The axis of the anticline plunges 26° N53W. The axial trend was determined from a plot of poles to limbs on a PI diagram (Fig. 10). Although the axial plane was not

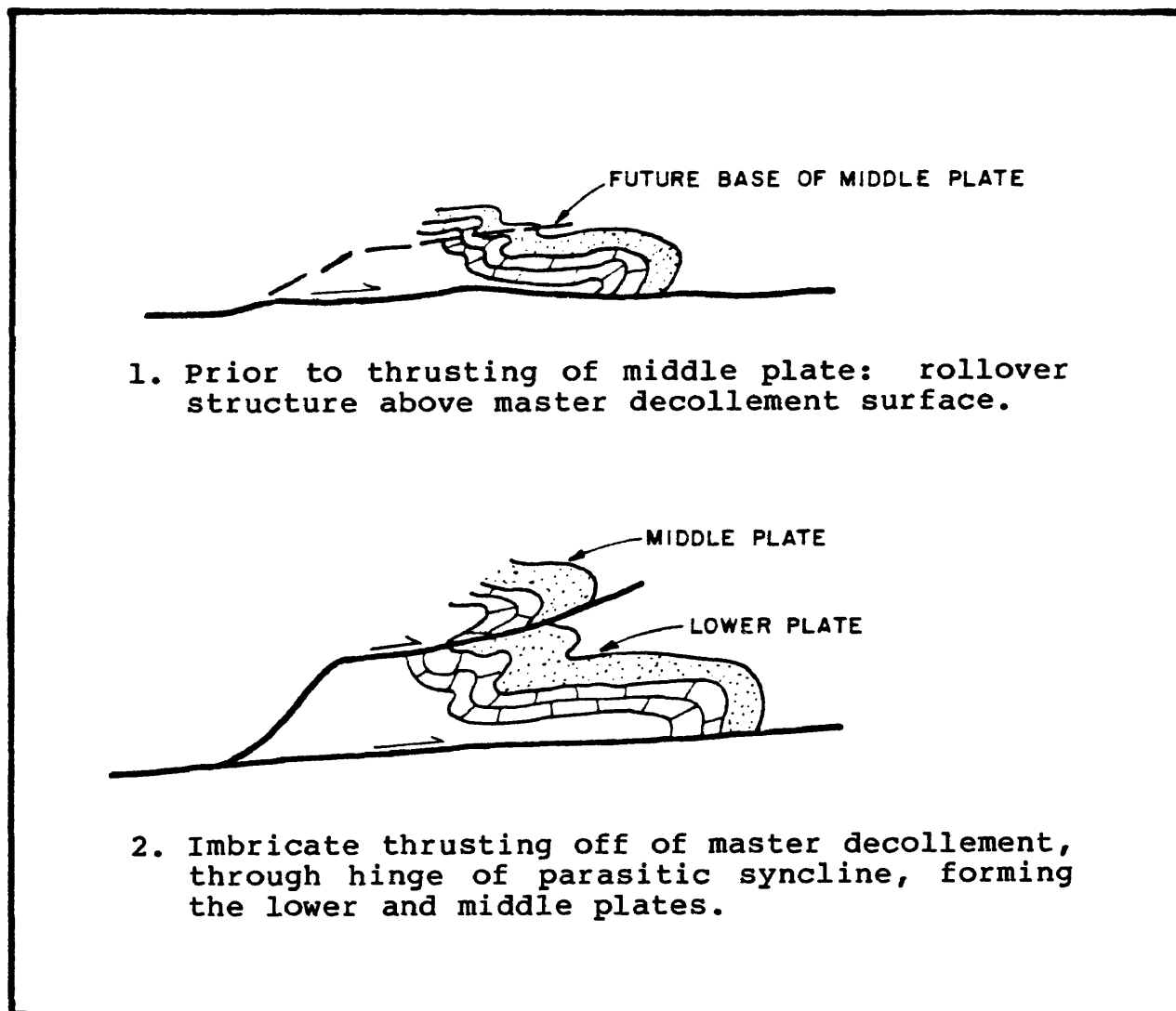


Figure 8. Schematic depiction of postulated development of the thrust fault separating the lower and middle plates.

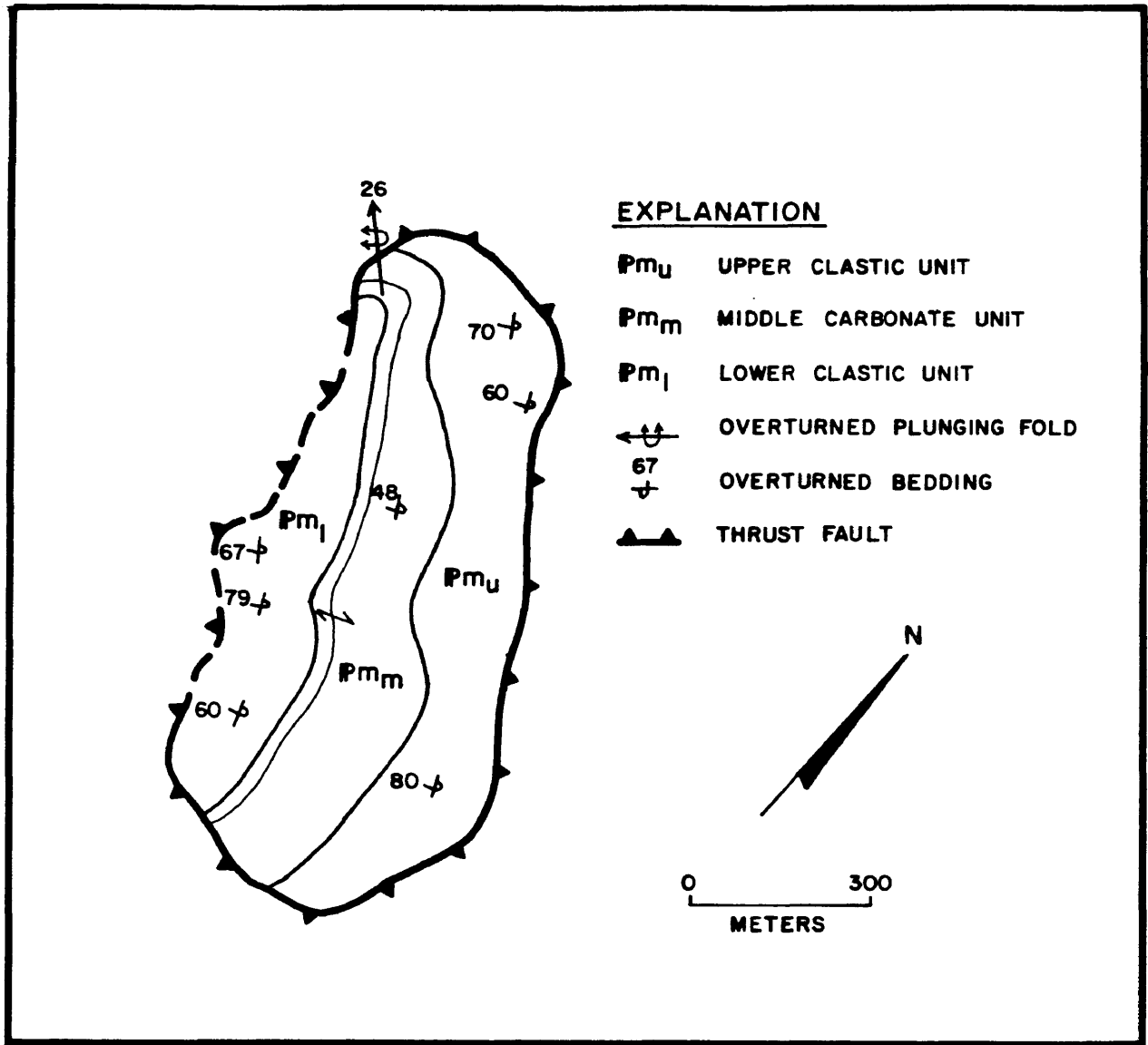


Figure 9. Lower plate geology exposed within the fenster.

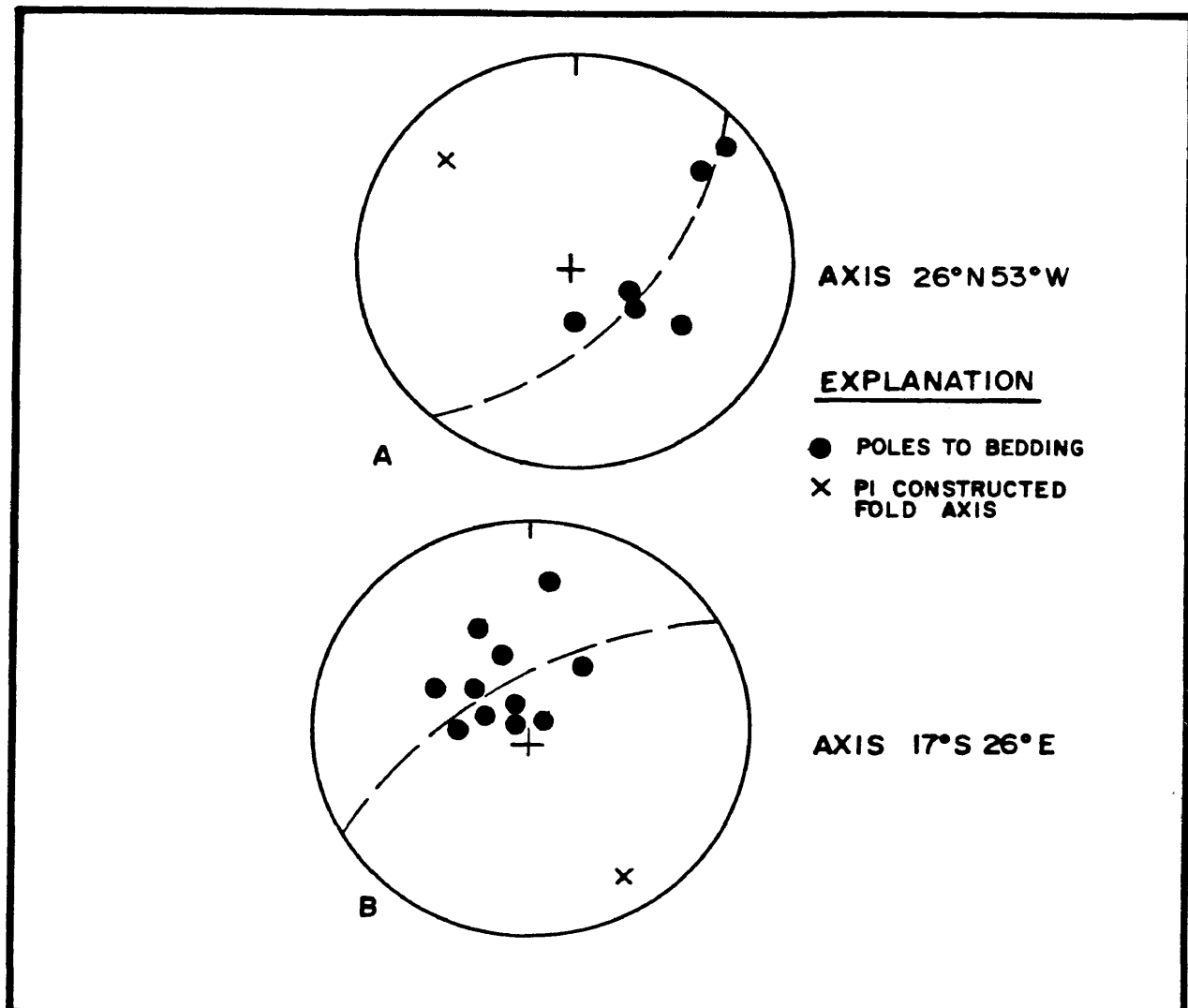


Figure 10. PI-diagrams of macroscopic folds in the study area.

- A. Overturned fold in the northwest corner of fenster.
- B. Antiformal syncline in the middle plate.

measurable in the field, it is estimated to trend north-northwest with a southwesterly dip.

Middle Plate

The middle plate is separated from the underlying plate by a low-angle thrust fault. Rocks of the middle plate are exposed over much of the field area and contain the most abundant structural data related to the thrusting. Strata within the plate include all three units of the Minturn Formation. Rocks trend north-northwest and dip either upright and steeply to the east, or are overturned and dip to the west (Pls. I and III). The dips change along strike due to minor folding in the less competent beds. The major structure within the middle plate is a large, inclined anticline. The limbs have been offset by a series of nearly vertical tear faults, and by a large reverse fault in the northeast (Pl. II).

Thrust Faults

The leading edge of the thrust fault between the lower and middle plates is not exposed in the field area. The topographic scarp along the eastern margin of the field area could, however, mark this boundary (cross-sections D-D' and C-C', Plate I). Where the fault surface trace is exposed, it

defines the periphery of the fenster. The fact that beds in the middle plate are overturned to the west suggests drag associated with thrust faulting. It is interpreted that this thrust fault dips gently to the west throughout most of the field area, although locally it dips to the east (Fig. 11).

Within the middle plate, a small thrust cuts the overturned limb of the major anticline (Pl. I, cross section C-C', location a). This is one of possibly several imbricate thrust faults associated with minor downcutting of the major thrust fault separating the lower and middle plates. Drag along the fault creates an antiformal syncline (Fig. 11). This small structure extends for only 472 meters (1,500 feet) and is only 122 meters (400 feet) wide. The hinge of the antiformal syncline plunges $17^{\circ}\text{S}26\text{E}$. This was determined by a PI diagram (Fig. 10).

Another small thrust is present in the hinge of the same major anticline (Pl. I, location b). The presence of the fault is inferred because of the double thickness of the middle carbonate unit in the hinge area (Fig. 12). Displacement is only observed in the hinge region of the fold.

Reverse Faults

A macroscopic reverse fault is present in the northeastern portion of the field area (Pl. I and cross section

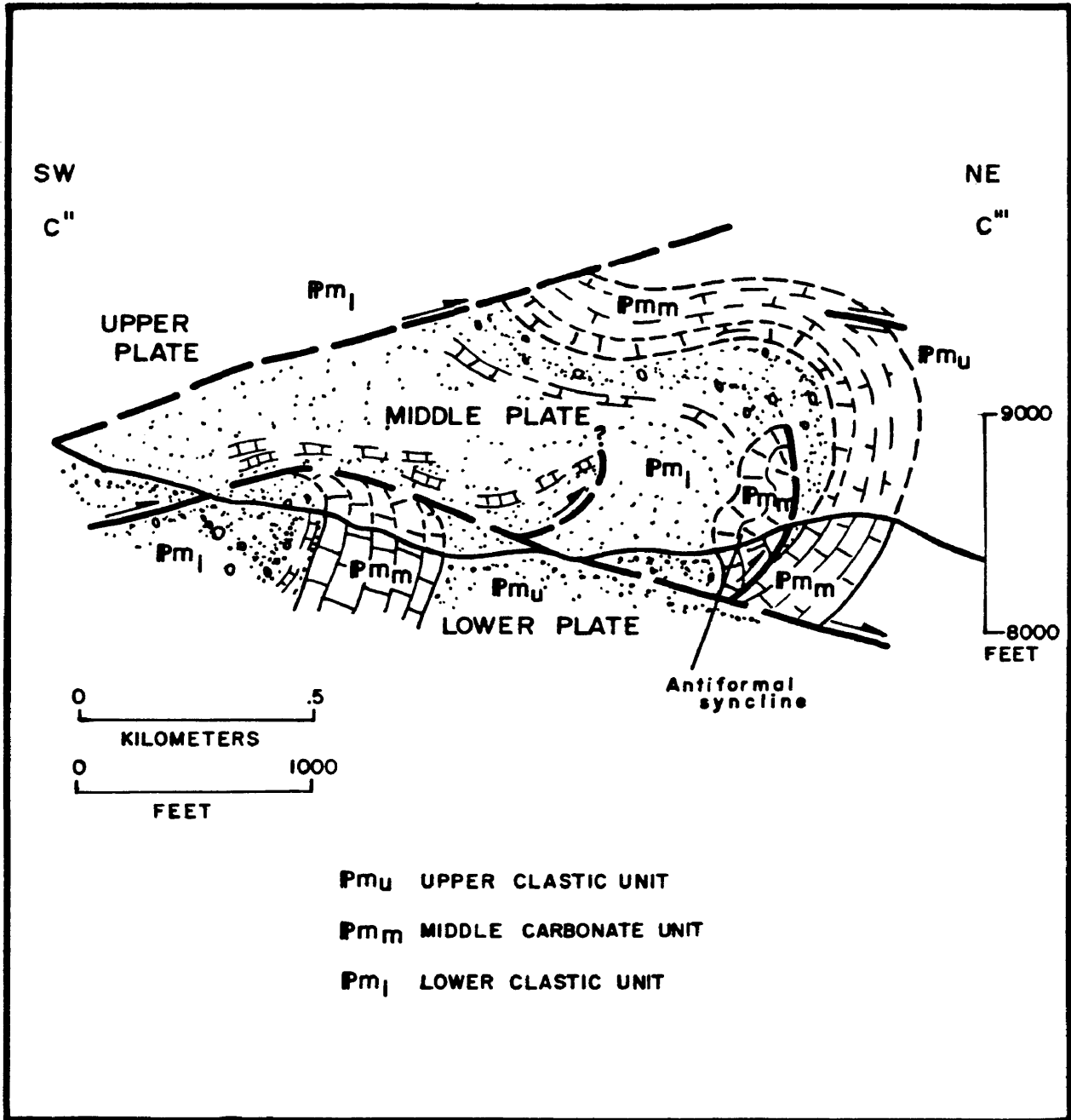


Figure 11. Breakage on the overturned limb within the middle plate forming an antiformal syncline (from Plate I, cross section C-C').

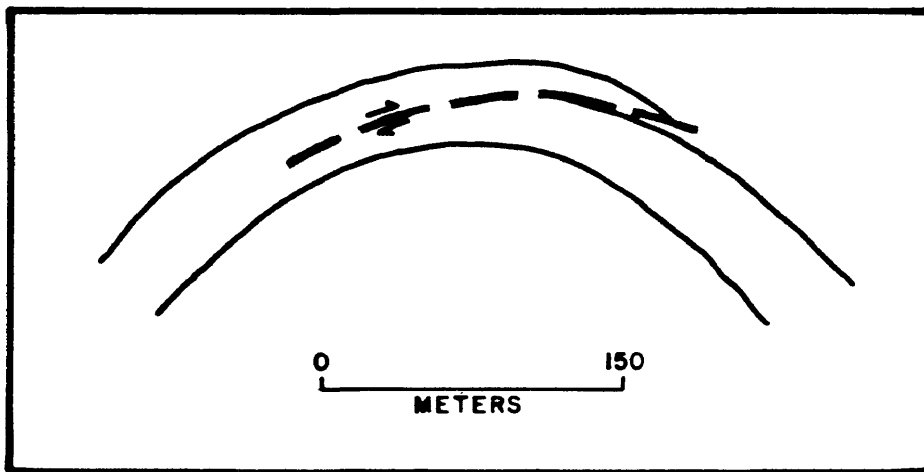


Figure 12. Schematic cross section exemplifying the style of thrusting within a fold hinge (from Perry, 1975).

D-D'). The fault dips steeply to the east. Along this fault the east-dipping upper clastic unit is structurally overlain by rocks of the middle carbonate unit also dipping to the east near the contact (Pl. III). This reverse fault is truncated by the upper thrust plate. The fault is interpreted to be a high-angle back-thrust along the major thrust. The high-angle fault probably formed late during the major thrust movement, but prior to emplacement of the upper thrust plate.

Tear Faults

Several small, map-scale, tear faults are present within, and possibly confined to, the middle thrust plate (Pl. I). They trend east-west and have displacements that vary from a few meters to tens of meters. The reverse fault in the northern part of the middle plate is cut by the northernmost tear fault (Pls. I and II, location c). These faults were probably formed as a result of differential movement within the middle plate as it rode over irregularities in the lower plate, such as the fenster area if it was structurally high during thrusting. Alternatively, tear faults could be related to a hidden buttress to the east.

Folds

Folds within the middle plate include a large, inclined anticline and macroscopic folds parasitic to the major anticline (Pls. I and II). Folding and faulting are believed to be contemporaneous deformational features. However, the folding may slightly precede some of the faulting. As horizontal compression is initiated, rocks often deform into folds prior to breakage in the hinges or along the short limb of the fold couple. Minor folds within the plates may post-date the faulting.

The inclined to overturned anticline within the middle plate can be traced throughout the eastern portion of the field area (Pl. II). The fold plunges northwest and exposes older rocks in the core to the south. PI-diagrams show that the trend of the fold axis ranges from N60-70W and that it plunges 15-30 degrees to the northwest and locally southeast (Fig. 13). The fold varies from an open to closed geometry. The mechanism of folding was probably a combination of flexural slip and flexural flow as the more ductile, shaly beds flow, and the more competent, sandstone and limestone beds show little ductile deformation and break by thrusting in the hinge regions of the folds.

To the west, farther from the leading edge of the middle plate, upright to inclined open folds trending northwest-

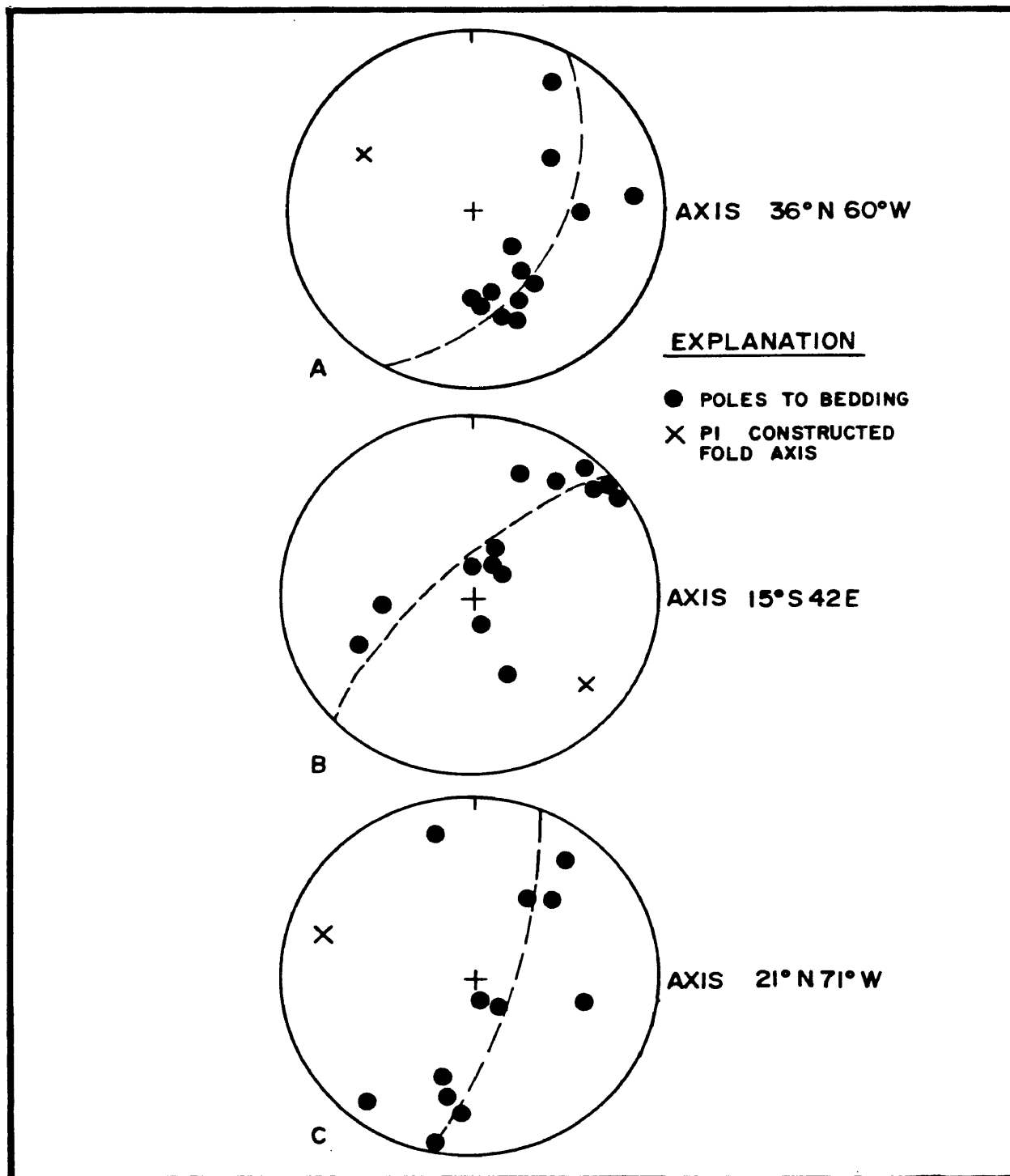


Figure 13. PI-diagrams of the macroscopic inclined to overturned anticline in middle plate.
 A. Middle carbonate unit in north-central portion of study area (Plate II).
 B. & C. Lower clastic unit in lower-eastern portion of study area (Plate II).

southeast can be traced in the lower clastic unit (Pl. I, location d and cross section B-B'). The folds are identified by bedding attitude changes within the upper clastic unit (Pl. III).

Small, northwest-trending parasitic folds can be traced along the overturned limb of the major anticline in the eastern portion of the field area (Pl. I, locations e and f). Viewed to the north, the movement sense is counterclockwise.

Along the strike of the overturned limb within the middle plate, the middle carbonate unit and the upper clastic unit locally fold in a torsional manner (Fig. 14). These propellar-like folds may be the result of a shearing component which occurred during thrusting. Because of poor outcrop exposure, these folds could not be measured quantitatively. However, the map pattern, and changes in dip along strike, generally outline the folds (Pls. I and III, location g).

Upper Plate

The upper plate has been thrust over the lower and middle plates, and is exposed in the western portion of the field area (Pls. I and II). The upper plate contains only rocks of the lower clastic unit. Very little internal structure was found due to the lack of stratigraphic markers

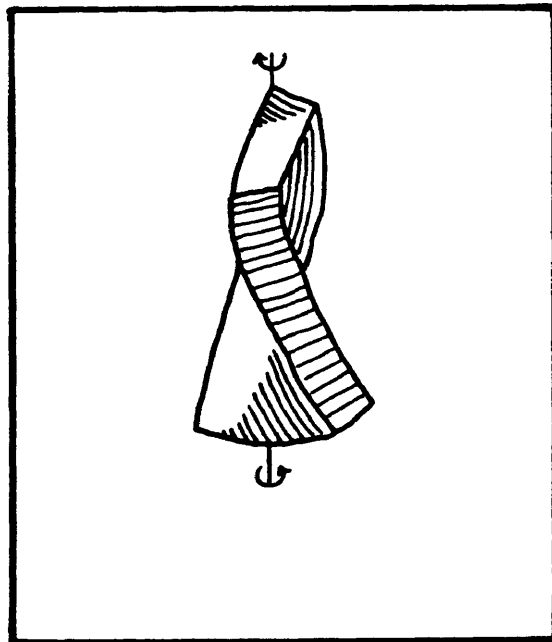


Figure 14. Propeller-like folding caused by torsional forces (from Billings, 1972).

within the lower clastic unit of this plate. However, sedimentary structures, such as cross-bedding and graded bedding, indicate that the strata are upright. Dips vary from nearly horizontal to moderately steeply dipping (up to 50 degrees) to the west.

Thrust Faults

The thrust fault contact between the middle and upper thrust plates, although poorly exposed, can be traced in the field in the northern portion of the area (Pl. I). The southern extension has been inferred on the geologic map and is projected in a longitudinal structure section (Fig. 15). The fault could not be accurately mapped in the southern part of the field area due to lack of outcrop. Dips of 13-15 degrees to the southwest along the fault contact were determined by three-point problem solutions. The thrust is interpreted to be a large splay off a lower décollement surface. Along the northern portion of the thrust fault separating the middle and upper plates, there is a small allochthonous block which is interpreted to be a small melange block transported along the fault plane during the thrusting event (Pl. I, location h).

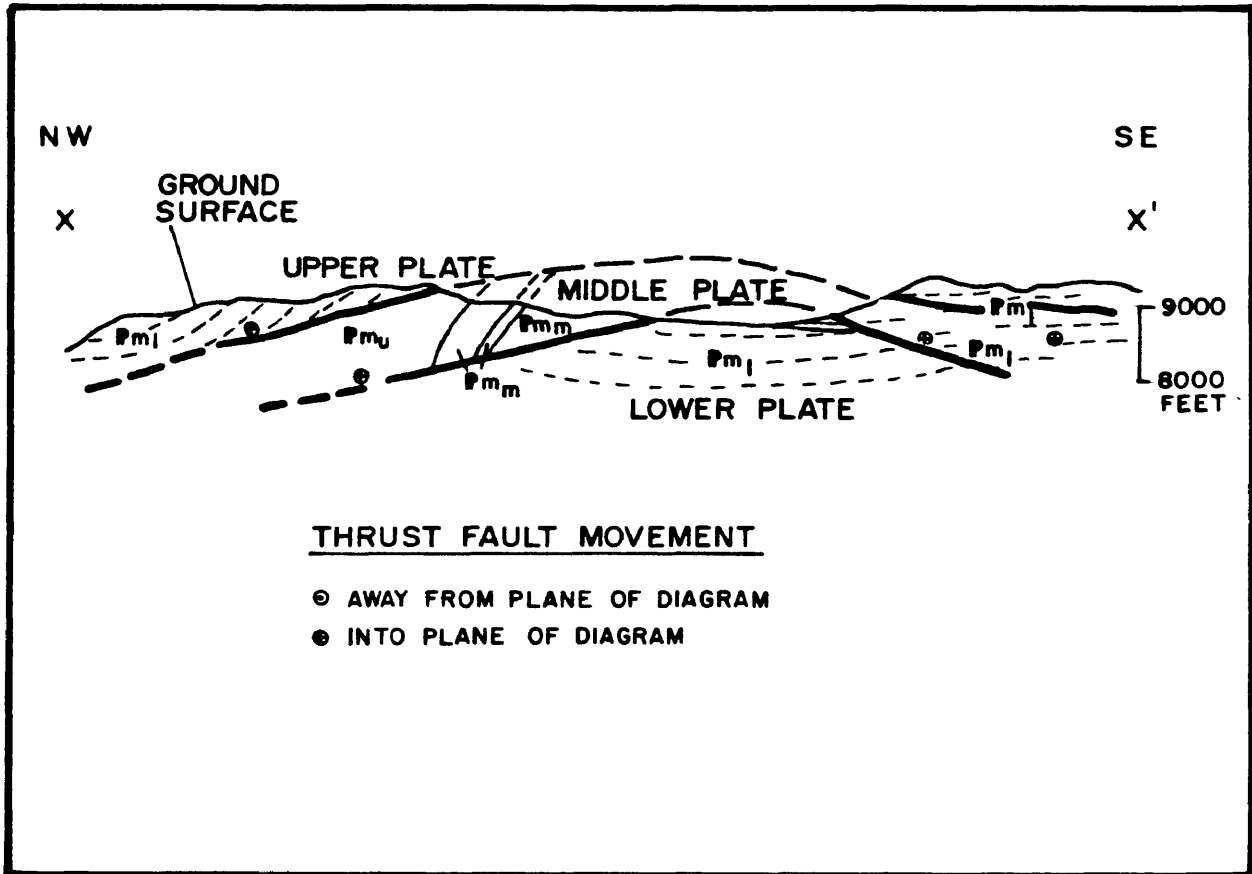


Figure 15. Longitudinal section X-X' from Plate I.

Folds

A large, open syncline is present within the upper plate. The fold was identified by changes in bedding attitudes. The fold axis, based on a PI diagram construction, plunges 10 degrees in the S13E direction (Fig. 16).

Summary

Two major thrust faults and associated structures were mapped in the field area. The thrust surfaces dip 5-15 degrees west and locally east. Minor, transverse, high-angle faults offset the thrust faults along strike. Major folds are interpreted to be inclined to overturned near the leading edge of the thrusts, and become open and diminish in amplitude to the west. Minor thrust faults are present in the hinge regions of some anticlines. Axes of thrust-related folds plunge gently and trend between N10W-N60W. The direction of thrust transport is interpreted to be from southwest to northeast, or perpendicular to the major fold axial trends.

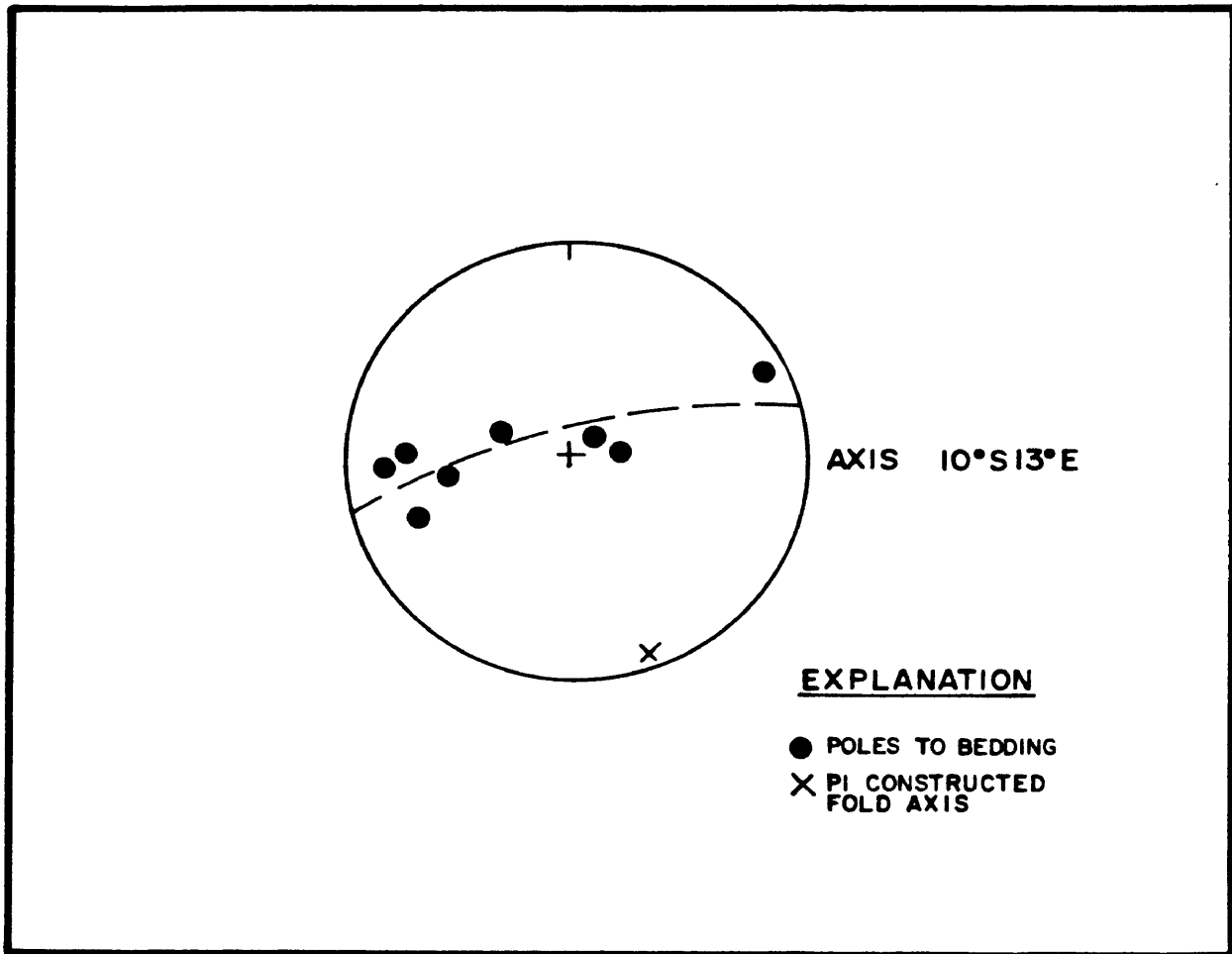


Figure 16. PI-diagram of macroscopic open syncline in upper plate.

Mesoscopic Structural Features

Introduction

Mesoscopic structural features include thrusts, folds, joints, high-angle faults, and slickensides. Orientation data are presented on a series of equal-area net projections (Pl. IV). The study area is divided into seven structural domains such that the mesoscopic structural features have similar orientation characteristics within a given domain. Trends of the mesoscopic structures are nearly the same as the macroscopic structures, inferring that they are both related to the same origin.

Mesoscopic Thrusts

Mesoscopic thrust offsets show transportation from west to east. The thrusts generally strike parallel to the bedding (N40E-N40W) and are horizontal or dip slightly to the west. Bedding-plane thrusts were noted in the middle and upper plates (Pls. II and IV). Brittle deformation is present in the more competent sandstones and limestones within the three units of the Minturn Formation (Fig. 17). Minor anticlines, or rollover structures, are present near the inferred ramping edges of the mesoscopic thrusts. In areas where the bedding-plane thrusts could be traced over one

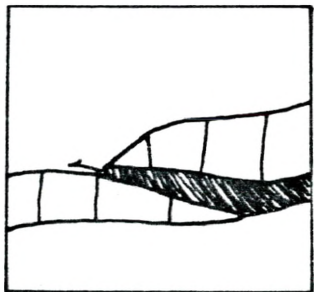


Figure 17. Photograph of a mesoscopic thrust fault in the middle carbonate unit (looking south).

hundred meters, the thrusts climb up section to the east. The bedding-plane thrusts were found near the major thrust faults and in the hinges of the major folds.

Folds

Mesoscopic folds are abundant in some portions of the field area. The less-competent lithologies have a similar style of folding, whereas the competent layers have a parallel style. The highest density of mesoscopic folds is near the major thrust faults and in the overturned folds in the eastern portion of the area within the middle plate.

Fold axes trend from N60W to north-south and plunge 5-60 degrees northwest or southeast. Most axial planes strike N30W-N30E and dip from horizontal to 80 degrees. The scatter in the data may be caused by differential movement within the thrust plates.

The sense of asymmetry of mesoscopic folds on the limbs of major folds is consistent with an origin related to shear within the limbs of the major folds. However, the asymmetry of mesoscopic folds related to deformation near major fault surfaces shows no consistency. These fault-related mesoscopic folds may be related to small shear zones within the different plates.

In summary, the style of folding varies with lithologic competency. The mechanism of folding varies from flexural-slip in the competent beds where constant bedding thickness is maintained (Fig. 18), to semi-similar folding within the less competent beds, where thinning in the limbs occurs and the overall fold dies down or up in section perpendicular to the fold hinge. Ramsey (1962) states that

"The geometry of these folds would appear to conform with the theoretical conditions of flexure folds, except that there appears to be some modification near the fold hinges which is almost certainly the result of flattening" (Fig. 19).

High-Angle Faults

The attitudes of mesoscopic, high-angle faults are plotted as poles to planes on a series of equal area nets (Pl. IV). Within each domain reverse and normal faults are distinguished. The determination of fault types is based on field observations including drag sense along the fault planes and appatent displacement of beds (Fig. 20). The mesoscopic faults have throws ranging from a few centimeters to a few meters.

The reverse faults trend north-south to N45W and dip from 60-90° southwest. The faults are found in the competent middle carbonate unit and in sandstone layers of the lower and upper clastic units. The lower and middle plates are cut



Figure 18. Photograph of a mesoscopic fold in the middle carbonate unit.

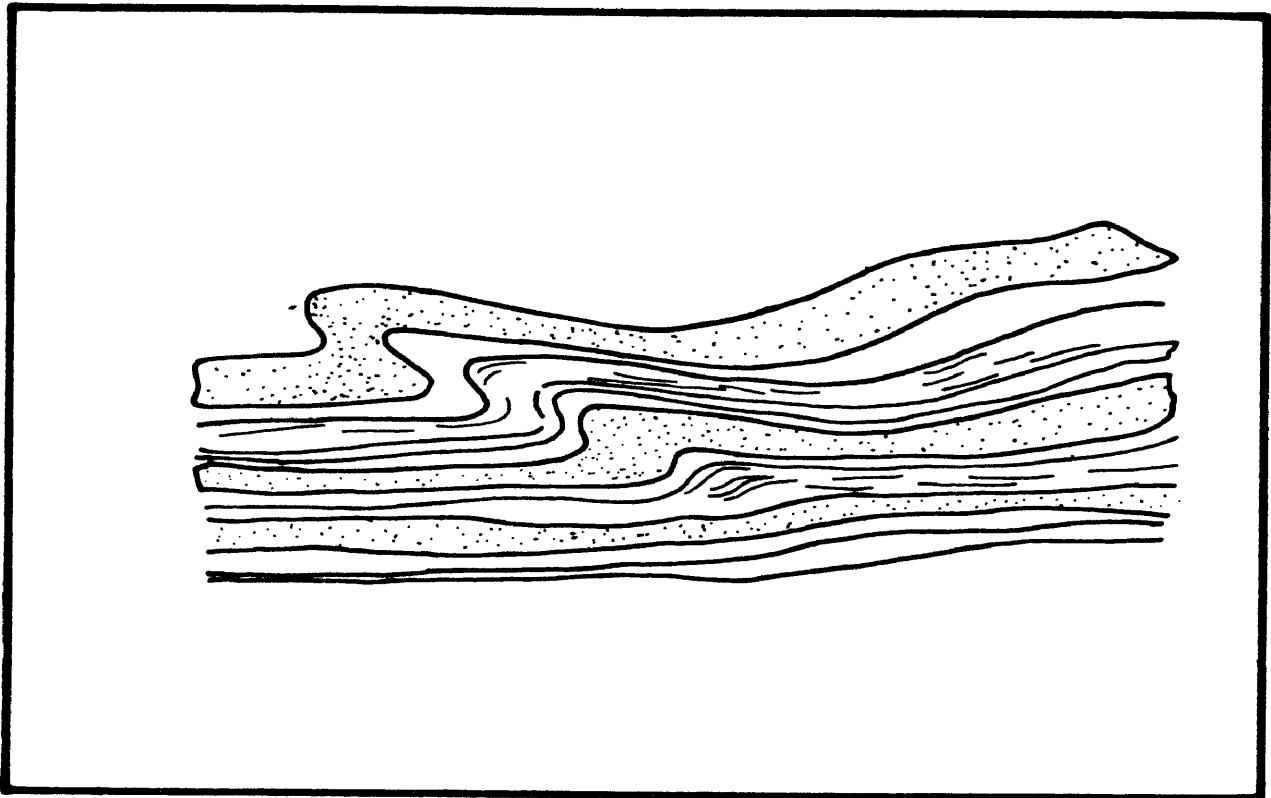


Figure 19. Modified flexural or semi-similar fold where mechanism is flexural slip but flattening modifications result from varying thicknesses and competencies (modified from Ramsey, 1962).



Figure 20. Photograph of drag along a mesoscopic normal fault in the middle carbonate unit (looking north).

by mesoscopic reverse faults in areas of major folding and faulting. The trends of the mesoscopic reverse faults are parallel to the major fold hinge traces and are perpendicular to the assumed direction of thrust movement. The mesoscopic reverse faults are parallel to the major reverse fault in the field area (Pl. II).

Mesoscopic normal faults which trend north-south to N40E are present throughout the field area (Pl. IV). These faults cut the low-angle, bedding-plane thrust faults. Throws on the mesoscopic normal faults range from a few centimeters to a meter. The normal faults are believed to have formed during a phase of relaxation or extension after the main thrusting occurred.

Joints

Two prominent sets of joints have been identified (Pl. IV). One set trends northwest-southeast and the other set trends northeast-southwest. The northeast-southwest set, unlike the other set, is filled with calcite suggesting that the two sets were formed during separate events. It has been stated that a joint analysis relating the formation or deformation of joints with a tectonic event requires a detailed joint analysis of the undeformed foreland. Price (1967) states

"It would appear that the thrusting and folding which are characteristic of the Rocky Mountains have not been a prerequisite for the development of joints. Many presumably formed before the more conspicuous large-scale orogenic structures, and under different stress conditions."

In light of the fact that the joints in this study were measured in a tectonically deformed, small area, the following inferences are speculative.

The northwest-trending joints are parallel to the hinge planes of the mesoscopic and macroscopic folds and are parallel to the trends of the mesoscopic reverse faults. It is suggested that the northwest-southeast joint set is related to the compressional deformation in the area.

The northeast-trending joints are filled with calcite throughout the field area. This joint set is developed in all the major compressional structures in the study area. The northeast-southwest trend is parallel to the trend of the mesoscopic normal faults (Pl. IV). The normal faults and the calcite-filled joints may have formed contemporaneously during a post-compressional relaxation or extensional event.

Slickensides

Slickenside lineations are plotted on equal-area nets for each domain (Pl. IV). The slickenside data were measured on high-angle fault planes. There are two distinguishable

clusters: one trends approximately N30W and plunges 45-85 degrees to the northwest and southeast, and the other cluster trends N20-45E plunging 30-80 degrees to the northeast and southwest. The northwest trending slickensides are interpreted to be related to the movement on mesoscopic reverse faults. Northeast trending slickensides are believed to be related to movement on mesoscopic normal faults. Most of the lineations plunge at very high angles (45-85 degrees) implying a dominantly dip-slip motion. The scatter (10-40 degree plunges) may be due to an oblique component of slip along some of the fault planes.

Summary

Mesoscopic structures include small bedding-plane thrusts, folds, reverse faults, normal faults, joints, and slickensides. Bedding-plane thrusts and mesoscopic fold axes suggest transport from the southwest to the northeast. Two sets of high-angle fault planes are distinguished: a northwest-southeast-trending set and a northeast-southwest-trending set. The northwest-southeast set consists of mesoscopic reverse faults, and the northeast-southwest set consists of normal faults. Mesoscopic normal faults cut mesoscopic thrusts. Two sets of joints with similar trends are also distinguished. The northeast-southwest-trending joint

set has calcite filling, whereas the northwest-southeast set does not. The calcite-filled joints cut thrusts, folds, and reverse faults. This may indicate a post-compressional relaxation or extension. Slickenside data indicates a dominantly dip-slip movement on the mesoscopic high-angle faults.

Microfabrics

Thin sections from oriented samples within the middle carbonate unit (Fig. 21) were studied to determine the amount of strain developed on the microscopic scale. The samples were taken from hinges and associated limbs of minor folds within the different thrust plates. Two or three thin sections, cut at right angles, were made from each of the oriented samples.

The middle carbonate unit was studied because there are oolitic beds within the unit. Oolites are useful as strain markers because they are assumed to be spherical before deformation (Hobbs et al., 1976). It was hoped that a consistent pattern of strain within the oolitic grainstone could be established. Upon thin section analysis, however, no measurable finite strain was observed. In thin section, the oolites are diagenetically altered, but the cross-sectional circular shape does not show a consistent strain pattern.

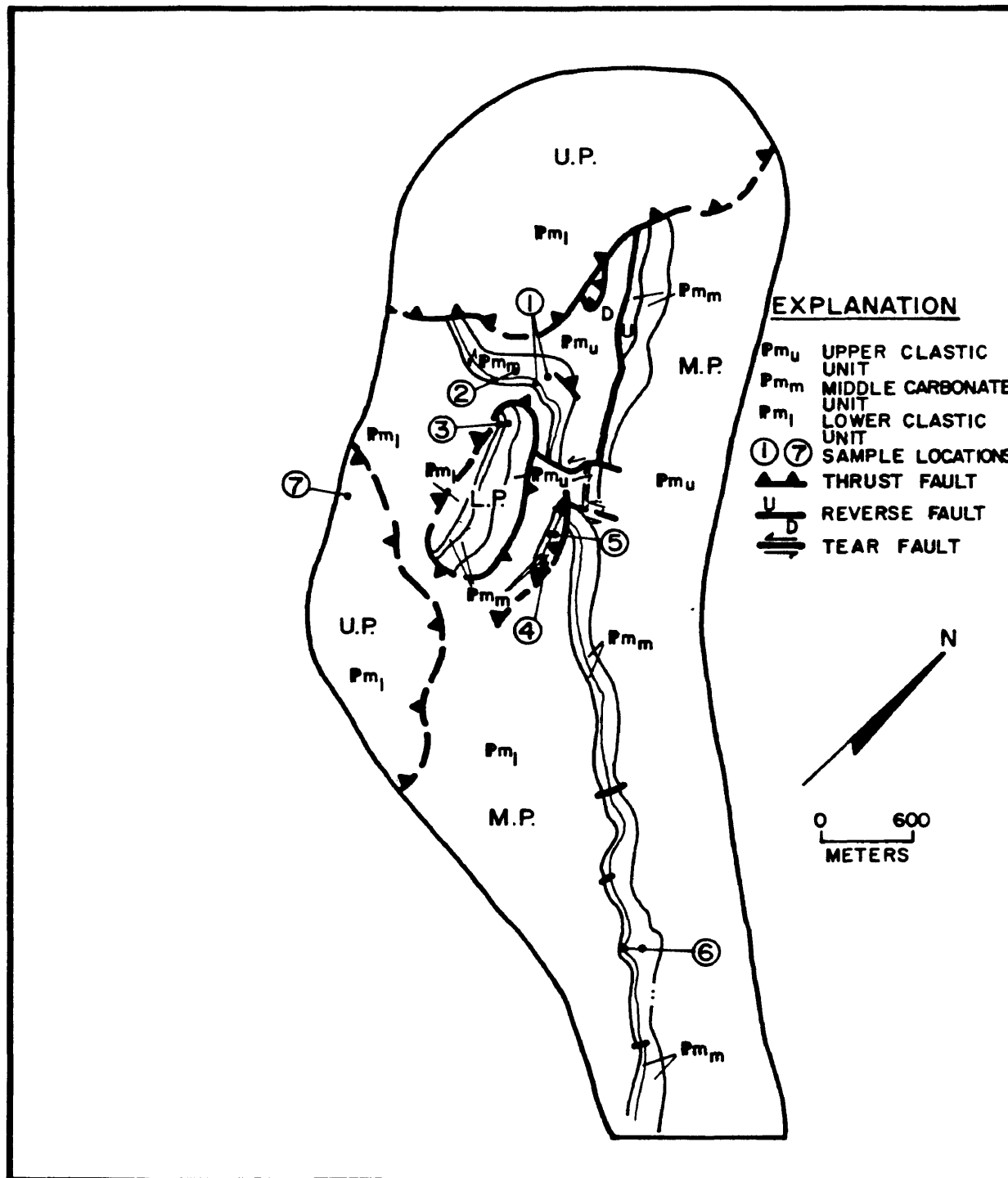


Figure 21. Locations of petrographic samples.

Petrographic descriptions and diagenetic alterations of the limestone facies are summarized in Table 1.

Table 1. Petrographic Descriptions of Limestones in the Lower Clastic and Middle Carbonate Units.

Sample 1

Fossiliferous (crinoids, fusilinids, bryazoa, green algae, brachiopod spines, and shell fragments), lime packstone. Micrite matrix recrystallized to dolomite(?). Late silica filled veins crosscut depositional features.

Sample 2

Oolitic lime packstone. Oolites are recrystallized, possibly dolmitized, but undeformed. Matrix of coarse calcite, some calcite crystals are micritized. Late calcite veins, and locally some late silica filled veins cut oolites.

Sample 3

Fossiliferous (brachiopods, bryazoa, crinoids, and brachiopod spines), lime packstone. Recrystallized micrite matrix, and crinoid fragments.

Sample 4

Fossiliferous (bryazoa, brachiopods, crinoids, and brachiopod spines) lime packstone. Recrystallized micrite matrix with crosscutting calcite filled veins.

Sample 5

Fossiliferous (crinoids, blue-green algae, pelecypod fragments, and bryazoa) lime packstone to wackestone. Recrystallized micrite matrix, and crinoid fragments. Late calcite veins crosscut fossil fragments.

Sample 6

Oolitic lime grainstone. The sample is completely recrystallized and the oolites are relict ghost structures (Scholle, 1978). There is no apparent deformation.

Sample 7 (from lower clastic unit)

Oolitic, fossiliferous (algae and echinoids) lime grainstone. Echinoid fragments are in the nucleus of the oolites. There is fibrous cementation around the peripheries of the oolites.

MODEL FOR THE GENESIS OF STRUCTURES

The structures in the study area are believed to be the result of a Late Cretaceous-Eocene (Laramide) compressional event affecting the Sangre de Cristo Range. The model presented here considers only the Paleozoic and Mesozoic sedimentary rocks of the Huerfano Park area (Fig. 6). Determining the timing of the development of structures in such a small area, and without the aid of dated intrusions or fore-deep sequences, is purely speculation. Wiltschko and Dorr (1983) used thrust-derived sediments to date the timing and displacement of major structures in the Wyoming Overthrust Belt and foreland. This type of dating is not applicable in an area as small as this study area, and the model proposed here is based on models from the Wyoming Overthrust Belt (Boyer and Elliot, 1982; Royse et al., 1975), the Canadian Rocky Mountains (Dahlstrom, 1977), and the Appalachian Mountains (Perry, 1978). These fold and thrust belts show similar structures to the study area.

During Laramide time, compression caused large blocks to move eastward along decollement surfaces within the sedimentary package (Fig. 22-A). The stratigraphy of the study area includes only a small portion of the Pennsylvanian section, therefore the horizon along which the detached plate glides

is not known. The field area is interpreted to be underlain by part of a master decollement surface. Based on a model with similar structures, the decollement is interpreted to ramp up east of the field area, and may generate large scale duplex structures near the ramping zone (Royse, Warner, and Reese, 1975).

Formation of folds occur as imbricated thrust faults develop along the decollement surface (Fig. 22-B). The fault surface propagates up section with associated rollover and local overturning due to drag along the thrust surface. Folding decreases in amplitude up section.

During thrusting, secondary, high-angle, transverse tear faults develop parallel to the transportation direction due to disparate displacement within the thrust plate (Dahlstrom, 1977). These tear faults are usually confined to individual thrust sheets.

Minor imbrications develop within the thrust plate along the leading edge or ramping zone (Dahlstrom, 1977), and possibly in an anomolous area where the thrust may locally cut down in section (Fig. 11). The direction of transportation is dominantly to the east, but backthrusting in the ramping zone does occur. After, or during, this imbrication phase, the beds west of the imbricate ramp warp into large, open folds (Plate I, location d).

The major, overturned and inclined anticlines observed in the lower and middle plates (Plate II) are interpreted to be rollover structures developed contemporaneously with thrusting. It is believed that minor curvilinear thrusts in the hinge areas of these folds are contemporaneous with the formation of the folds (Perry, 1978).

The structural geology of this small, eight square km area reflects similar large-scale structures observed in the Wyoming Overthrust Belt. It is implicit in the proposed model that the sequential development of large structures, as documented by Dahlstrom (1977), Boyer and Elliot (1982), Wiltschko and Dorr (1983), and numerous others, is similar to the development of folds and thrusts in the study area. The development of normal faults and extension joints post-dates the compressional event.

Regionally, Precambrian rocks to the west have been interpreted to be allochthonous (Lindsey et al., 1983). This suggests that the Sangre de Cristo Range represents a zone of Laramide crustal shortening. East-west compression in the Rocky Mountain foreland has been suggested by Smithson and others (1979) and Brown (1982). More recently, Gries (1983) suggests a change from east-west to north-south compression during the Laramide orogeny. The southwest-northeast trans-

port direction suggested in this study advocates a compressional model.

Vertical block uplifts generating compressional structures along their flanks (Matthews, 1976) may be a feasible, alternate model for the structures observed in this study. Gravity sliding along a major decollement surface above the basement is another mechanism proposed for the development of thrust faults in the Sangre de Cristo Range (Karig, 1964). The proposed existence of allochthonous Precambrian basement (Lindsey et al., 1983) creates problems with this overall model. Locally, however, thrust faults may have formed as a result of small-scale gravity slides. Regional transcurrent movement during Laramide time (Sales, 1968) may have produced compressional features, however a regional study is necessary to correlate the structural features mapped in the study area to a transcurrent model.

Due to the small size of the study area, it is impossible to interpret a regional model. Nevertheless, this study implies that during Laramide time a compressional regime existed in the Huerfano Park area. The sedimentary rocks folded and faulted in a classic overthrust style, thus implying a zone of crustal shortening. A compressional model is supported, but vertical or transcurrent models can not be excluded as working hypotheses.

CONCLUSIONS

Three units within the Pennsylvanian Minturn Formation underlie the area west of the town of Chama. The lower clastic unit is a cyclic fan-delta deposit consisting of interbedded arkosic conglomerate, arkosic sandstone, and siltstone, and arkosic to quartzose limestone. The middle carbonate unit is a shelf-carbonate sequence consisting of a basal argillaceous, fossiliferous lime packstone rich with Dictyoclostus brachiopods. It is overlain by fossiliferous lime packstone and wackestone, and oolitic grainstone. The upper clastic unit represents a shallow-marine, delta-fringe environment. It contains interbedded, thinly-bedded, sandstone, siltstone and limestone.

Laramide-age forces have folded and faulted the rocks in a geometric style similar to the Wyoming fold and thrust belt. There are three imbricate thrust plates that overlap one another in the field area. Along the thrust contacts, dips range from 5-15 degrees to the west and locally to the east. Transportation was from southwest to northeast. Differential stress within the thrust plates occurred during emplacement, resulting in the development of minor high-angle tear faults. Folding occurred contemporaneously with, and as a result of, thrusting. Major, map-scale folds show an over-

turned style that becomes open and diminishes in amplitude to the west. Locally, minor thrust faults develop in the hinge areas of anticlines.

Mesoscopic structures formed under the same deformational conditions as the macroscopic structures in the area. Small bedding thrusts indicate shortening in the southwest-northeast direction. Parasitic folds have axial traces perpendicular to the direction of transport.

A model for the genesis of structures is as follows: A major compressional event during the Laramide orogeny transported the rocks in the field area along a major decollement surface. The package of rocks broke into a series of imbricate thrusts. Associated folding, minor thrusting, back thrusting, and tear faulting occurred simultaneously. Minor normal faults are related to a later relaxation or extensional event.

REFERENCES CITED

- Bagg, R.M., Jr. 1908, Some copper deposits in the Sangre de Cristo Range, Colorado: *Econ. Geology*, v. 3, n. 8, p. 739-749.
- Billings, M.P., 1972, *Structural Geology*, Prentice-Hall Inc., Englewood, N.J., 3rd edition, 513 p.
- Bolyard, D.W., 1959, Pennsylvanian and Permian stratigraphy in the Sangre de Cristo Range between La Veta Pass and Westcliffe, Colorado: *Am. Assoc. Petroleum Geologist Bull.*, v. 43, n. 8, p. 1896-1939.
- Boyer, S.E., and Elliot, D., 1982, Thrust Systems: *Am. Assoc. Petroleum Geologist Bull.*, v. 66, n. 9, p. 1196-1230.
- Briggs, L.I., and Goddard, E.N., 1956, *Geology of Huerfano Park, Colorado: Guidebook to the geology of the Raton Basin, Colorado*, Rocky Mountain Assoc. of Geologists, p. 40-45.
- Brill, K.G. Jr., 1952, Stratigraphy in the Permo-Pennsylvanian zeugeosyncline of Colorado and northern New Mexico: *Geol. Soc. America Bul.*, v. 63, p. 809-880.
- Brown, W.G., 1983, Sequential development of the fold-thrust model of foreland deformation: *Rocky Mountain Foreland Basins and Uplifts*, Rocky Mountain Assoc. Geologists, 1983, p. 57-65.
- Burbank, W.S., and Goddard, E.N., 1937, Thrusting in Huerfano Park, Colorado, and related problems of orogeny in the Sangre de Cristo Range: *Geol. Soc. America bull.*, v. 48, n. 7, p. 931-976.
- Burford, A.E., 1960, *Geology of the Medano Peak area, Sangre de Cristo Range, Colorado*: PhD thesis, Univ. Michigan, Ann Arbor, Mich., 201 p.
- Clarke, R.F., 1982, Stratigraphy, sedimentology, and copper-uranium occurrences of the upper part of the Middle Pennsylvanian Minturn Formation: M.S. thesis, Colorado School of Mines, Golden, Co. 150 p.

- Clement, J.F., 1952, The geology of the northeastern Baca Grand area, Saguache county, Colorado: M.S. thesis, Colorado School of Mines, Golden, Co. 128 p.
- Dahlstrom, C.D.A., 1977, Structural geology in the eastern margin of the Canadian Rocky Mountains: Wyoming Geol. Assoc. Guidebook, 29th annual field conf., p. 407-439.
- Dixon, J.S., 1982, Regional structural synthesis, Wyoming salient of western overthrust belt: Am. Assoc. Petroleum Geologists Bull., v. 66, n. 10, p. 1560-1580.
- De Voto, R.H., and Peel, F.A., 1972, Pennsylvanian and Permian stratigraphy and structural history, northern Sangre de Cristo Range, Colorado, in De Voto, R.H., ed., Paleozoic stratigraphy and structural evolution of Colorado: Colorado School of Mines Quart., v. 67, n. 4, p. 283-320.
- De Voto, R.H., 1980, Pennsylvanian stratigraphy and history of Colorado, in Colorado Geology: Rocky Mountain Assoc. Geologists Symposium.
- Donath, F.A., and Parker, D.B., 1964, Folds and folding: Geol. Soc. America Bull., v. 75, p. 45-62.
- Emmons, S.F., 1898, Ten Mile District special folio, Colorado: Geol. Atlas of U.S. folio 48.
- Endlich, F.M., 1874, Report of F.M. Endlich, in Hayden, F.V., Progress report of exploration for the year 1873, Annual Report of the United States Geological and Geographical Survey of the Territories, embracing Colorado, p. 275-351.
- Gableman, J.W., 1952, Structure and origin of northern Sangre de Cristo Range, Colorado: Am. Assoc. Petroleum Geologist Bull., v. 36, n. 8, p. 1574-1612.
- Greis, Robbie, 1983, North-south compression of Rocky Mountain foreland structures: Rocky Mountain Foreland Basins and Uplifts, Rocky Mountain Assoc. Geologists 1983, p. 9-33.
- Hobbs, B.E., Means, W.D., and Williams, P.F., 1976, An outline of structural geology, John Wiley and Sons Inc., N.Y., 571 p.

- Johnson, J.H., 1929, Contribution to the geology of the Sangre de Cristo Range of Colorado: Colorado Sci. Soc. Proc., v. 12, n. 1, p. 1-21.
- Johnson, R.B., 1960, Geology of the Huerfano Park area, Huerfano and Custer counties, Colorado: U.S.G.S. Bull. 1071-D, p. 87-119.
- Karig, D.H., 1964, Structural analysis of the Sangre de Cristo Range, Venerable Peak to Crestone Peak, Custer and Saguache counties, Colorado: M.S. thesis, Colorado School of Mines, Golden, Colorado, 143 p.
- Lindsey, D.A., Clarke, R.F., Soulliere, S.J., and Flores, R.J., 1984, Minturn and Sangre de Cristo Formations of southern Colorado—a prograding fan-delta and alluvial-fan sequence shed from the Ancestral Rocky Mountains: In press.
- Lindsey, D.A., Johnson, B.R., and Andriessen, P.A.M., 1983, Laramide and Neogene structure of the northern Sangre de Cristo Range, south-central Colorado: Rocky Mountain Foreland Basins and Uplifts, Rocky Mountain Assoc. Geologists 1983, p. 219-229.
- Litsey, L.R., 1958, Stratigraphy and structure of the northern Sangre de Cristo Range, Colorado: Geol. Soc. America Bull., v. 69, n. 9, p. 1143-1178.
- Matthews, V. III, 1976, Mechanism of Laramide deformation along the northeastern flank of the Colorado Front Range, in Epis, R.C., and Weimer, R.J., eds., Studies in Colorado field geology, Prof. Contrib. Colorado School of Mines, n. 8, p. 398-402.
- Munger, R.D., 1965, Structural geology of the Spread Eagle Peak area, Sangre de Cristo Range, Colorado: Mountain Geologist, v. 2, n. 5, p. 1054-1068.
- Perry, W.J. Jr., 1978, Sequential deformation in the central Appalachians: American Journal of Science, v. 278, p. 518-542.
- Pierce, W.H., 1969, Geology and Pennsylvanian-Permian stratigraphy of howard area, Fremont county, Colorado: M.S. thesis, Colorado School of Mines, Golden, Colorado, 129 p.

- Price, R.A., 1967, The tectonic significance of mesoscopic subfabrics in the southern Rocky Mountains of Alberta and British Columbia: Canadian Journal of Science, v. 4, p. 39-70.
- Ramsey, J.G., 1962, The geometry and mechanics of formation of "similar type folds: Journal of Geology, v. 70, p. 309-327.
- Royse, F., Warner, M.A., and Reese, D.L., 1975, Thrust belt structural geometry and related stratigraphic problems Wyoming-Idaho-northern Utah: Rocky Mountain Assoc. Geologists Symp., p. 41-52.
- Sales, J.K., 1968, Crustal mechanics of foreland deformation: A regional and scale model approach: Am. Assoc. Petroleum Geologists Bull. v. 52, n. 10, p. 2016-2044.
- Scholle, P.A., 1978, Carbonate rock constituents, textures, cements, and porosities: Am. Assoc. Petroleum Geologist Memoir 27, 241 p.
- Smith, Russell, 1961, The geology of the Redwing area, Huerfano county, Colorado: PhD thesis, Univ. Michigan, Ann Arbor, Mich., 143 p.
- Smithson, S.B., Brewer, J.A., Kaufman, S., Oliver, J.E., and Hurich, C.A., 1979, Structure of Laramide Wind River uplift, from COCORP deep reflection data and from gravity data: Jour. Geophys. Research, v. 84, n. B11, p. 5955-5972.
- Stearns, D.W., 1978, Faulting and forced folding in the Rocky Mountains foreland: Geol. Soc. America Mem. 151 p.
- Taranik, J.V., 1974, Stratigraphic and structural evolution of Breckenridge area, central Colorado: PhD thesis, Colorado School of Mines, Golden, Colorado, 222 p.
- Tischler, H., 1961, The Pennsylvanian and Permian stratigraphy of the Huerfano Park area, Colorado: PhD thesis, Univ. Michigan, Ann Arbor, Mich. 201 p.
- Tweto, Ogden, 1975, Laramide (Late Cretaceous-Early Tertiary) orogeny in the Cenozoic history of the southern Rocky Mountains: Geol. Soc. America Mem. 144, p. 1-44.

Volkman, R.P., 1965, Geology of the Crestone Peak area, Sangre de Cristo Range, Colorado: PhD thesis, Univ. Michigan, Ann Arbor, Mich., 115 p.

Wiltschko, D.V., and Dorr, J.A. Jr., 1983, Timing of deformation in overthrust belt and foreland of Idaho, Wyoming, and Utah: Am. Assoc. Petroleum Geologist Bull., v. 67, n. 8, p. 1304-1322.

PLATE I GEOLOGIC MAP AND STRUCTURE SECTIONS

WESTERN HUERFANO PARK
HUERFANO COUNTY, COLORADO

by
GABRIELLE SCHAVRAN
1984
T2862



ARTHUR LAKES LIBRARY
COLORADO SCHOOL OF MINES
GOLDEN, COLORADO 80401

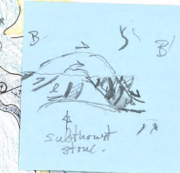
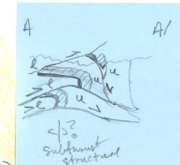
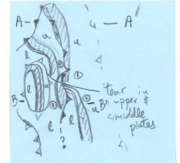
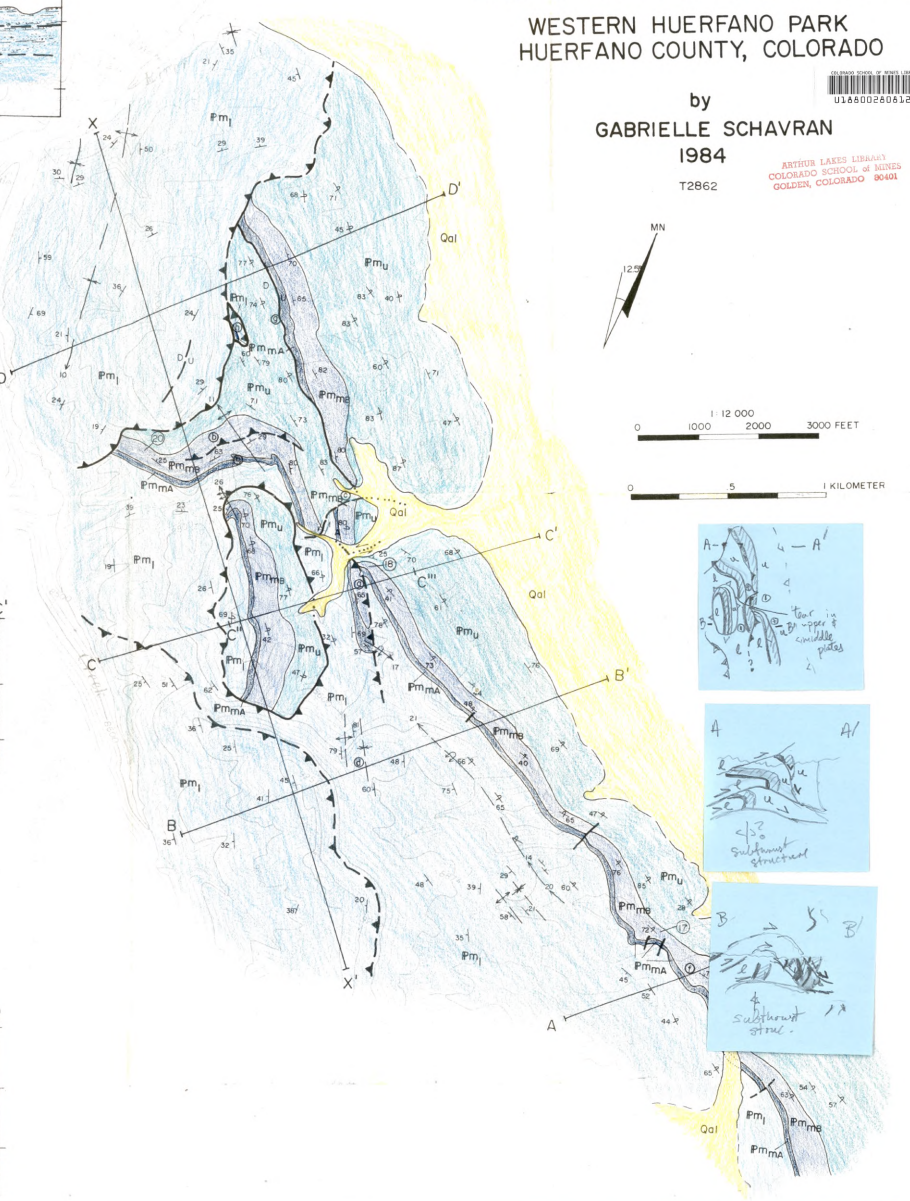
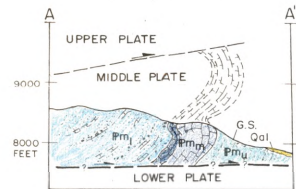
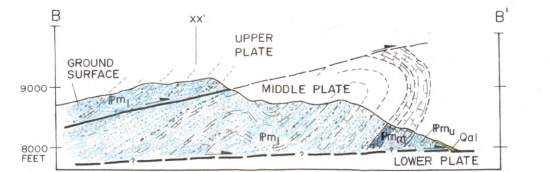
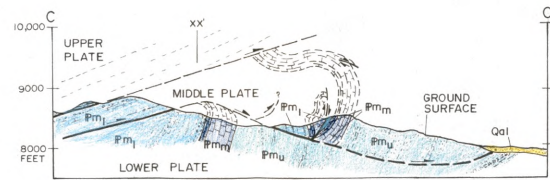
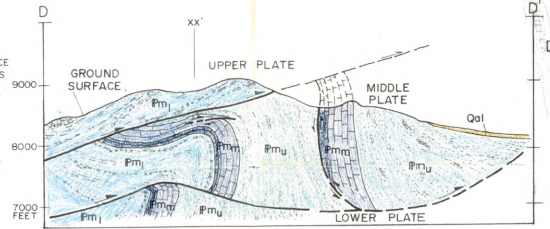
EXPLANATION

SYMBOLS

— CONTACTS	- - - INFERRED	↑ +	NON-PLUNGING ANTICLINE / SYNCLINE] HINGE SURFACE TRACES
▲ THRUST FAULT	▲ - - - INFERRED	10 +	PLUNGING ANTICLINE / SYNCLINE	
U / D	REVERSE FAULT	- - - - - INFERRED	10 +	OVERTURNED PLUNGING ANTICLINE / SYNCLINE
—	TEAR FAULT	- - - - - INFERRED	45	STRIKE AND DIP OF BEDDING
—	UNDIFFERENTIATED HIGH-ANGLE FAULT	67	VERTICAL BEDDING	
⊙ AWAY	THRUST FAULT MOVEMENT	+	VERTICAL BEDDING	
⊙ TOWARD	THRUST FAULT MOVEMENT	⊙ AWAY	INFERRED THRUST FAULT MOVEMENT	
AA' - DD'	STRUCTURAL SECTIONS	⊙ TOWARD	INFERRED THRUST FAULT MOVEMENT	
XX'	LONGITUDINAL STRUCTURAL SECTION	⊙	REFERENCE LOCATION	
		(17)	SPECIFIED FIGURE LOCATION	

STRATIGRAPHY OF THE UPPER MINTURN FORMATION

Qal	QUATERNARY ALLUVIUM
Pm _u	UPPER CLASTIC UNIT: INTERBEDDED GREEN, MICACEOUS SANDSTONE, BROWN, SILTY SANDSTONE, WHITE, LIMY SHALE AND SILTSTONE, BLACK SHALE WITH INTERBEDDED LIMESTONE WITH CHEST NODULES, TAN SANDSTONE, AND PINK AND GREEN ARKOSIC SANDSTONE
Pm _m	MIDDLE CARBONATE UNIT: MEMBER A: GREEN TO GRAY, ARGILLACEOUS, FOSSILIFEROUS LIME-PAKSTONE WITH DICTYOCLOSTUS BRACHIOPODS MEMBER B: FOSSILIFEROUS, GREEN TO GRAY, LIME-PAKSTONE, TAN SANDY LIME-WACKSTONE, FOSSILIFEROUS, LIME-PAKSTONE, OOLITIC, LIME-GRAINSTONE, AND LOCAL FACIES VARIATIONS
Pm _l	LOWER CLASTIC UNIT: INTERBEDDED PINK AND GREEN ARKOSIC CONGLOMERATE, GREEN, ARKOSIC SANDSTONE, ARKOSIC SILTSTONE, SANDY, ARKOSIC, LIMESTONE, AND CALCARENITE



EXPLANATION

SYMBOLS

- | | | | |
|--|--|--|----------|
| | CONTACT | | INFERRED |
| | THRUST FAULT | | INFERRED |
| | REVERSE FAULT | | INFERRED |
| | TEAR FAULT | | INFERRED |
| | UNDIFFERENTIATED HIGH-ANGLE FAULT SHOWING DIP OF FAULT PLANE | | |

- | | | | |
|--|------------------------------|--|---------------------------------------|
| | AWAY THRUST FAULT MOVEMENT | | AWAY INFERRED THRUST FAULT MOVEMENT |
| | TOWARD THRUST FAULT MOVEMENT | | TOWARD INFERRED THRUST FAULT MOVEMENT |

- REFERENCE LOCATION

- NON-PLUNGING ANTICLINE/SYNCLINE

- PLUNGING ANTICLINE/SYNCLINE

- OVERTURNED PLUNGING ANTICLINE/SYNCLINE

- STRIKE AND DIP OF BEDDING

- OVERTURNED BEDDING

- VERTICAL BEDDING

- A-A' D-D' STRUCTURE SECTIONS

- X-X' LONGITUDINAL STRUCTURE SECTION

HINGE SURFACE TRACES

STRATIGRAPHY

- | | |
|--|-----------------------|
| | QUATERNARY ALLUVIUM |
| | UPPER CLASTIC UNIT |
| | MIDDLE CARBONATE UNIT |
| | LOWER CLASTIC UNIT |

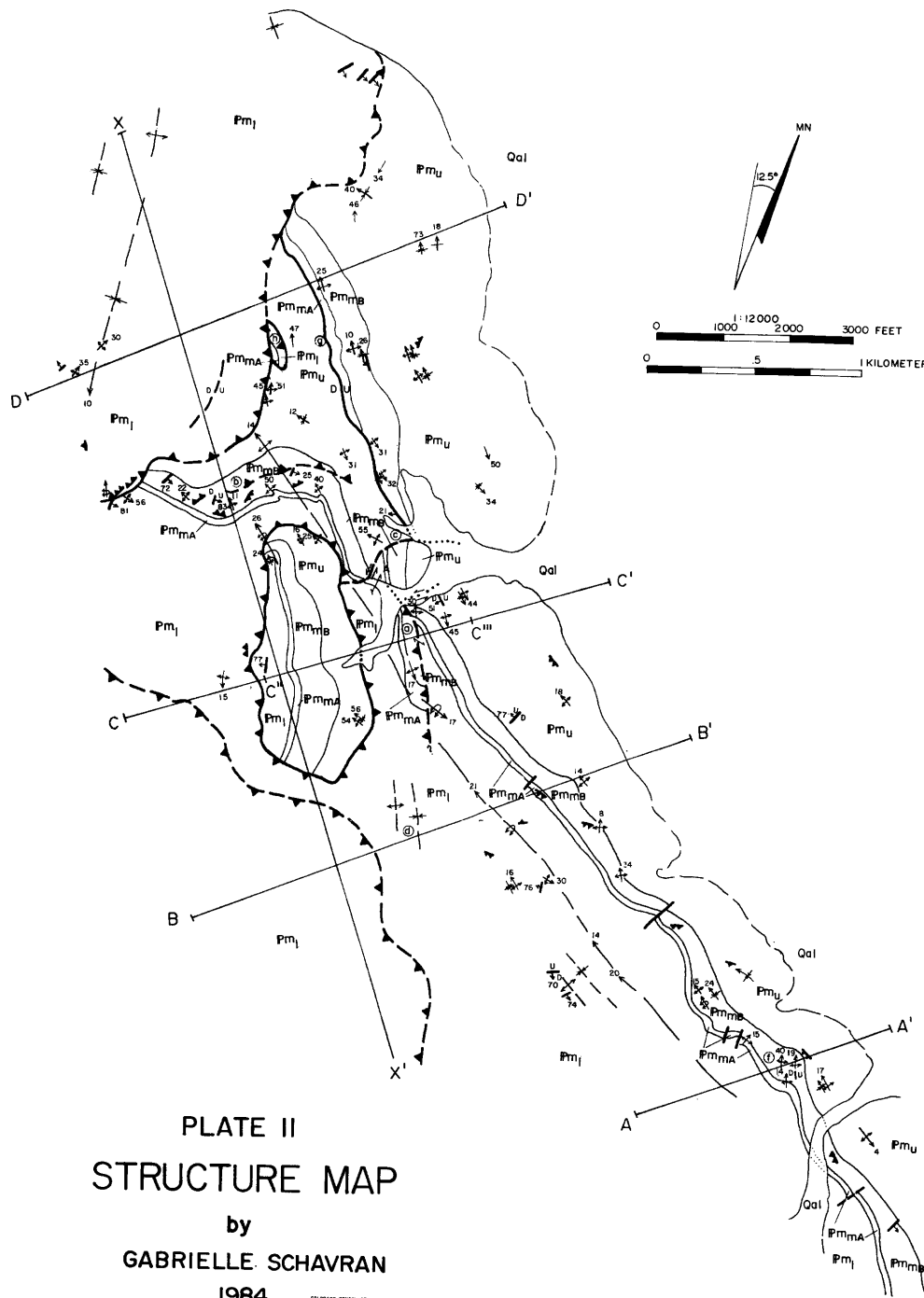


PLATE II STRUCTURE MAP

by

GABRIELLE SCHAVRAN

1984

T2862



EXPLANATION

SYMBOLS

	CONTACT		INFERRED
	THRUST FAULT		INFERRED
	REVERSE FAULT		INFERRED
	TEAR FAULT		INFERRED
	UNDIFFERENTIATED HIGH-ANGLE FAULT SHOWING DIP OF FAULT PLANE		

	AWAY THRUST FAULT MOVEMENT		AWAY INFERRED THRUST FAULT MOVEMENT
	TOWARD MOVEMENT		TOWARD INFERRED FAULT MOVEMENT

REFERENCE LOCATION

	NON-PLUNGING ANTICLINE/SYCLINE	HINGE SURFACE TRACES
	PLUNGING ANTICLINE/SYCLINE	
	OVERTURNED PLUNGING ANTICLINE/SYCLINE	
	STRIKE AND DIP OF BEDDING	
	OVERTURNED BEDDING	
	VERTICAL BEDDING	

A-A' - D-D' STRUCTURE SECTIONS

X-X' LONGITUDINAL STRUCTURE SECTION

STRATIGRAPHY

	QUATERNARY ALLUVIUM
	UPPER CLASTIC UNIT
	MIDDLE CARBONATE UNIT
	LOWER CLASTIC UNIT

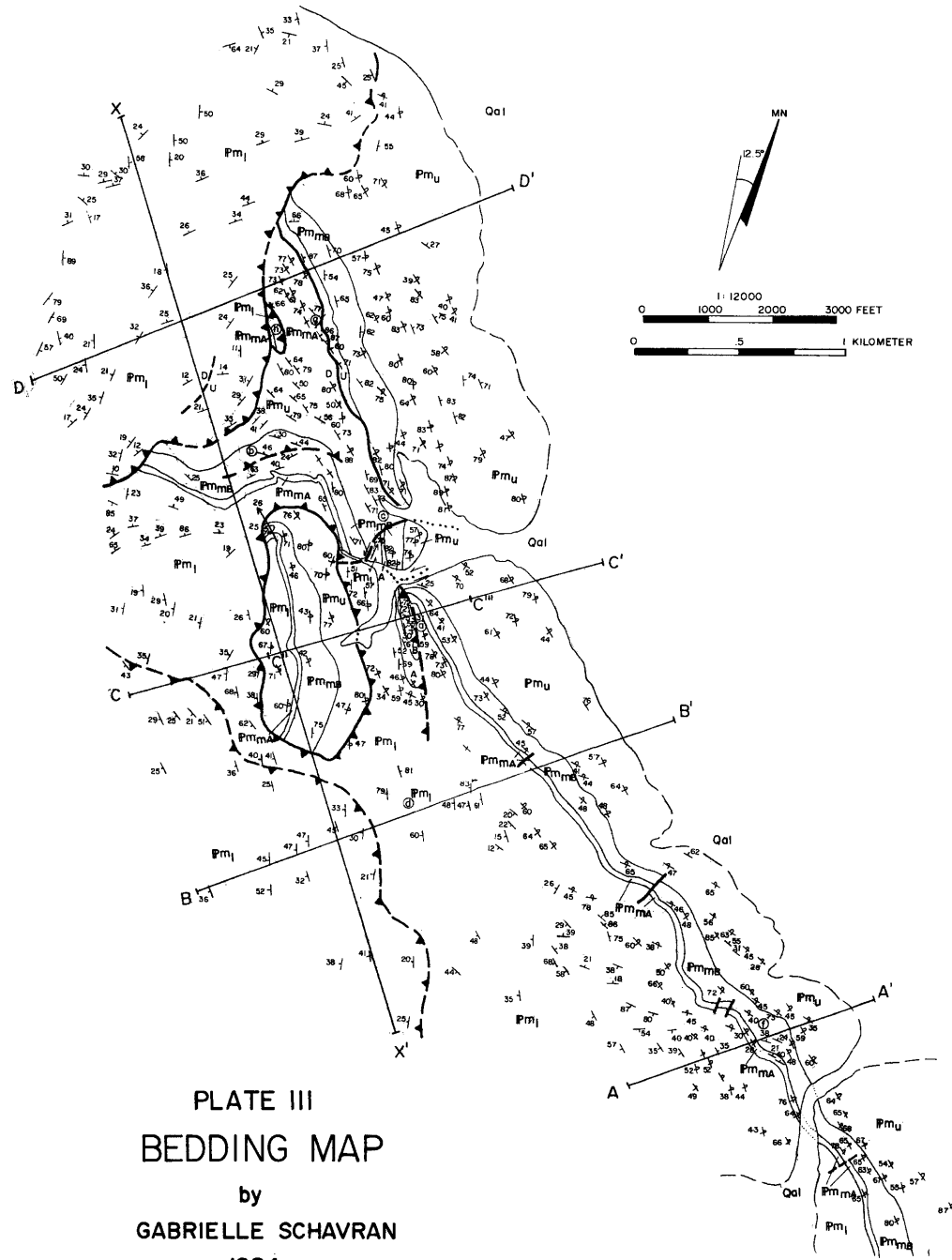


PLATE III BEDDING MAP

by
GABRIELLE SCHAVRAN

1984

T2862



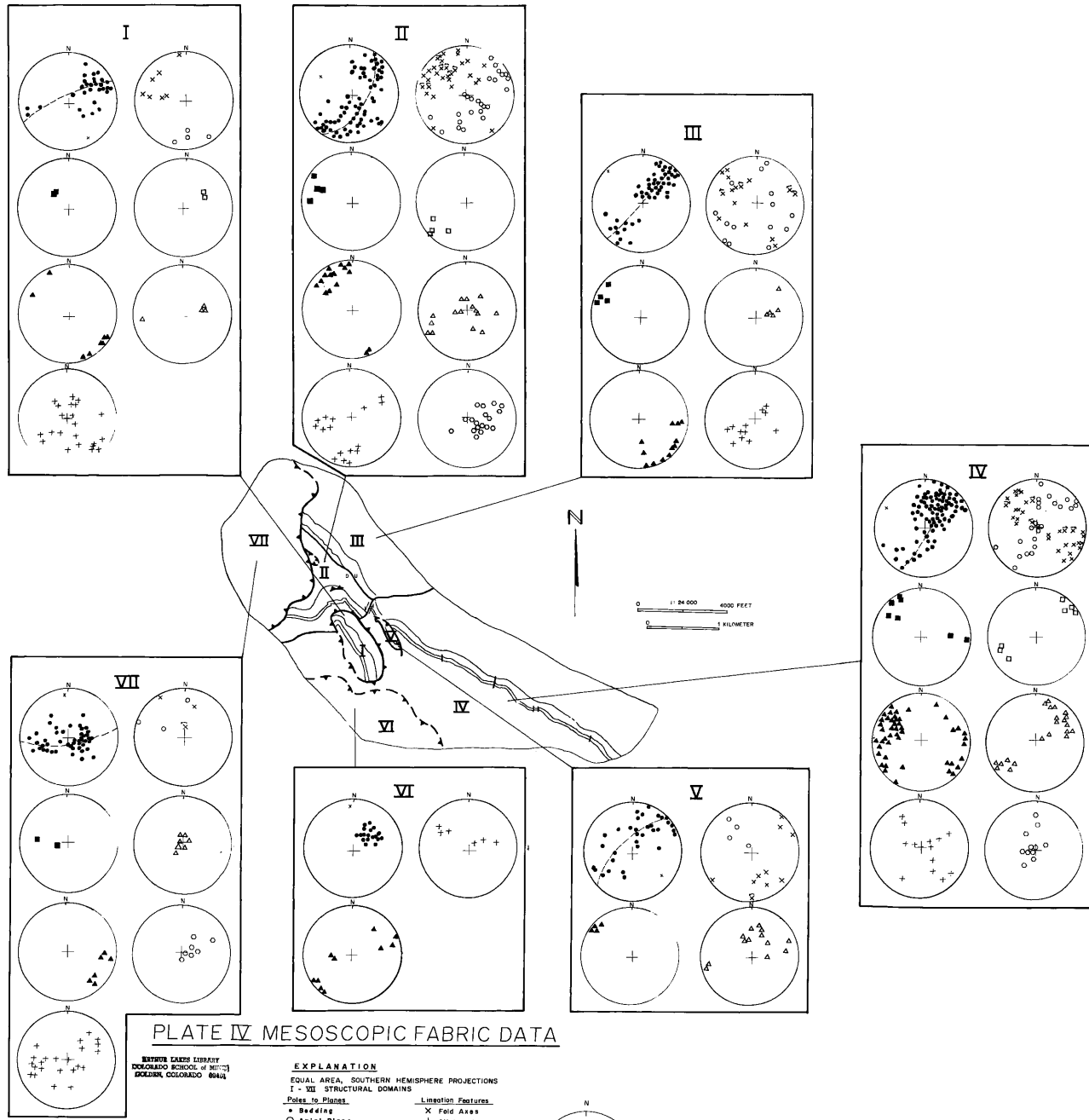


PLATE IV MESOSCOPIC FABRIC DATA

BYRON EAKS LIBRARY
 COLORADO SCHOOL OF MINES
 GOLDEN, COLORADO 80401

- EXPLANATION**
- EQUAL AREA, SOUTHERN HEMISPHERE PROJECTIONS
 I - VII STRUCTURAL DOMAINS
- Poles to Planes
- Bedding
 - Axial Planes
 - ◻ Reverse Fault
 - ◼ Normal Fault
 - ▲ Calcite-Filled Joint
 - ▲ Calcite-Filled Joint
 - Mesoscopic Thrust Faults
- Lineation Features
- X Fold Axis
 - + Slickensides
 - ~ Fold Asymmetry

by
 GABRIELLE SCHAVRAN
 1984
 T-2462